

1 **Ecological Controls on N<sub>2</sub>O Emission in Surface Litter and Near-surface**  
2 **Soil of a Managed Grassland: Modelling and Measurements**

3 Grant, R.F.<sup>1</sup>, Neftel, A.<sup>2</sup> and Calanca, P.<sup>2</sup>

4 <sup>1</sup> *Department of Renewable Resources, University of Alberta, Edmonton, AB, Canada T6G 2E3*

5 <sup>2</sup> *Agroscope Institute for Sustainability Sciences ISS, Reckenholzstrasse 191, P.O. Box CH – 8046*  
6 *Zürich, Switzerland*

7

8

**ABSTRACT**

9 Large variability in N<sub>2</sub>O emissions from managed grasslands may occur because most emissions  
10 originate in surface litter or near-surface soil where variability in soil water content ( $\theta$ ) and temperature  
11 ( $T_s$ ) is greatest. To determine whether temporal variability in  $\theta$  and  $T_s$  of surface litter and near-surface  
12 soil could explain that in N<sub>2</sub>O emissions, a simulation experiment was conducted with *ecosys*, a  
13 comprehensive mathematical model of terrestrial ecosystems in which processes governing N<sub>2</sub>O  
14 emissions were represented at high temporal and spatial resolution. Model performance was verified by  
15 comparing N<sub>2</sub>O emissions, CO<sub>2</sub> and energy exchange, and  $\theta$  and  $T_s$  modelled by *ecosys* with those  
16 measured by automated chambers, eddy covariance (EC) and soil sensors at an hourly time-scale during  
17 several emission events from 2004 to 2009 in an intensively managed pasture at Oensingen,  
18 Switzerland. Both modelled and measured events were induced by precipitation following harvesting  
19 and subsequent fertilizing or manuring. These events were brief (2 – 5 days) with maximum N<sub>2</sub>O  
20 effluxes that varied from  $< 1 \text{ mg N m}^{-2} \text{ h}^{-1}$  in early spring and autumn to  $> 3 \text{ mg N m}^{-2} \text{ h}^{-1}$  in summer.  
21 Only very small emissions were modelled or measured outside these events. In the model, emissions  
22 were generated almost entirely in surface litter or near-surface (0 – 2 cm) soil, at rates driven by N  
23 availability with fertilization vs. N uptake with grassland regrowth, and by O<sub>2</sub> supply controlled by litter  
24 and soil wetting relative to O<sub>2</sub> demand from microbial respiration. In the model, NO<sub>x</sub> availability  
25 relative to O<sub>2</sub> limitation governed both the reduction of more oxidized electron acceptors to N<sub>2</sub>O and the  
26 reduction of N<sub>2</sub>O to N<sub>2</sub>, so that the magnitude of N<sub>2</sub>O emissions was not simply related to surface and

27 near-surface  $\theta$  and  $T_s$ . Modelled  $N_2O$  emissions were found to be sensitive to defoliation intensity and  
28 timing which controlled plant N uptake and soil  $\theta$  and  $T_s$  prior to and during emission events. Reducing  
29 LAI remaining after defoliation to one-half that under current practice and delaying harvesting by 5 days  
30 raised modelled  $N_2O$  emissions by as much as 80% during subsequent events and by an average of 43%  
31 annually. Modelled  $N_2O$  emissions were also found to be sensitive to surface soil properties. Increasing  
32 near-surface bulk density by 10% raised  $N_2O$  emissions by as much as 100% during emission events and  
33 by an average of 23% annually. Relatively small spatial variation in management practices and soil  
34 surface properties could therefore cause the large spatial variation in  $N_2O$  emissions commonly found in  
35 field studies. The global warming potential from annual  $N_2O$  emissions in this intensively managed  
36 grassland largely offset those from net C uptake in both modelled and field experiments. However  
37 model results indicated that this offset could be adversely affected by suboptimal land management and  
38 soil properties.

39

40

## INTRODUCTION

41 The contribution of managed grasslands to reducing atmospheric greenhouse gas (GHG)  
42 concentrations through net uptake of  $CO_2$  (Ammann et al., 2005) may be at least partially offset by net  
43 emissions of  $N_2O$  (Conant et al., 2005, Flécharde et al., 2005). These emissions may be substantial, with  
44  $N_2O$  emission factors of as large as 3% measured in intensively managed grasslands with fertilizer rates  
45 of 25 - 30 g N m<sup>-2</sup> y<sup>-1</sup> (Imer et al., 2013; Rafique et al., 2011) These emissions are highly variable  
46 temporally and spatially because they are determined by complex interactions among short-term weather  
47 events (warming, precipitation), land management practices (N amendments, defoliation), and soil  
48 properties (e.g. bulk density, water retention). The  $N_2O$  driving these emissions in managed grasslands is  
49 thought to be generated within the upper 2 cm of the soil profile (van der Weerden et al., 2013) and in  
50 surface litter left by grazing or harvesting (Pal et al., 2013) so that diurnal heating and precipitation  
51 events that cause rapid warming and wetting of the litter and soil surface may cause large but brief  
52 emission events. These events are thought to be driven by increased demand for electron acceptors by  
53 nitrification and denitrification, and reduced supply of  $O_2$  by which these demands are preferentially  
54 met, and therefore increased demand for alternative acceptors  $NO_3^-$ ,  $NO_2^-$  and  $N_2O$  by autotrophic  
55 nitrifiers and heterotrophic denitrifiers.

56 The magnitude of N<sub>2</sub>O emission events in managed grasslands generally increases with the  
57 amount of N added as urine, manure or fertilizer, and with the intensity of defoliation by grazing or  
58 cutting (Ruzjerez et al. 1994). Thus Imer et al. (2013) found a negative correlation between LAI and  
59 N<sub>2</sub>O emissions at intensively managed grasslands in Switzerland. The increase in emissions with  
60 defoliation has been attributed to increased urine and manure deposition and soil compaction with  
61 defoliation by grazing, and to slower uptake of N and water by slower-growing plants with defoliation  
62 by harvesting (Jackson et al., 2015). Both N additions and defoliation are thought to raise these  
63 emissions by increasing the supply of NH<sub>4</sub><sup>+</sup> and NO<sub>3</sub><sup>-</sup> to autotrophic nitrifiers and heterotrophic  
64 denitrifiers. This increase raises the demand for alternative e<sup>-</sup> acceptors by these microbial populations if  
65 the supply of O<sub>2</sub>, the preferred e<sup>-</sup> acceptor, fails to meet demand, as may occur when soil water content  
66 ( $\theta$ ) after defoliation rises with precipitation or reduced transpiration. This supply is governed by physical  
67 and hydrological properties (porosity, water retention) of the near-surface soil. Consequently land use  
68 practices and soil properties must be considered when estimating N<sub>2</sub>O emissions from managed  
69 grasslands.

70 Recognition of the effects of precipitation events, N amendments and soil properties on N<sub>2</sub>O  
71 emissions has led to empirical models in which annual emission inventories are calculated directly from  
72 annual precipitation and N inputs (Lu et al., 2006), or monthly emission events are calculated from  
73 monthly precipitation, air temperature  $T_a$ , and  $\theta$  (Flécharde et al., 2007). However the soil depth at which  
74 most emitted N<sub>2</sub>O is generated (0 – 2 cm) is much shallower than that at which  $\theta$  used in these models is  
75 measured (5 – 10 cm) (Flécharde et al., 2007), and the soil temperature  $T_s$  at this depth may differ from  $T_a$   
76 This is particularly so for grasslands in which N additions are necessarily left on the soil surface without  
77 incorporation. Thus large N<sub>2</sub>O emissions may be caused by surface wetting from precipitation on dry  
78 soils following fertilizer application, so that deeper  $\theta$  is sometimes found to be of little explanatory value  
79 in empirical models (Flécharde et al., 2007). Furthermore the response of denitrification to  $\theta$  has been  
80 found in experimental studies to rise sharply with  $T_s$ , likely through the combined effects of  $T_s$  on  
81 increasing demand and reducing supply of O<sub>2</sub> at microbial microsites (Craswell, 1978). The interaction  
82 between  $T_s$  and  $\theta$  on N<sub>2</sub>O emissions is clearly apparent in the meta-analysis of N<sub>2</sub>O emissions from  
83 European grasslands by Flécharde et al. (2007). This interaction has been represented in empirical models  
84 by fitting interdependent threshold values of  $T_s$  and  $\theta$  above which emissions have been measured in  
85 field experiments (Smith and Massheder, 2014). However a more robust simulation of this interaction on

86 N<sub>2</sub>O emissions should be built from basic biological and physical processes that are independent of site-  
87 specific measurements.

88 Process models used to simulate N<sub>2</sub>O emissions from managed grasslands must therefore  
89 explicitly represent the effects of short-term weather events on near-surface  $T_s$  and  $\theta$ , as well as the  
90 effects of N additions and defoliation on near-surface  $\text{NH}_4^+$  and  $\text{NO}_3^-$ . These models must also  
91 explicitly represent the effects of mineral N,  $T_s$  and  $\theta$ , and of soil physical and hydrological properties,  
92 on the demand for vs. supply of O<sub>2</sub> and alternative e<sup>-</sup> acceptors  $\text{NO}_3^-$ ,  $\text{NO}_2^-$  and N<sub>2</sub>O, and on the  
93 oxidation-reduction reactions by which these e<sup>-</sup> acceptors are reduced. However earlier process models  
94 have usually simulated N<sub>2</sub>O emissions as  $T_s$ -dependent functions of nitrification and denitrification  
95 rates, modified by texture-dependent functions of water-filled pore space (WFPS) (e.g. Li et al., 2005).  
96 In some models additional empirical functions of  $T_s$  (Chatskikh et al., 2005), or of  $T_s$  and WFPS  
97 (Schmid et al., 2001), are used to calculate the fraction of nitrification that generates N<sub>2</sub>O, and the  
98 fraction of heterotrophic respiration  $R_h$  that drives denitrification (Schmid et al., 2001), thereby avoiding  
99 the explicit simulation of O<sub>2</sub> and its control on N<sub>2</sub>O emissions. A more detailed summary of functions of  
100 mineral N,  $T_s$  and WFPS currently used to model N<sub>2</sub>O emissions is given in Fang et al. (2015).  
101 These functions have many model-dependent parameters and function independently of each other, so  
102 that key interactions among reduced C and N substrates,  $T_s$  and  $\theta$  on N<sub>2</sub>O production may not be  
103 simulated. In none of these approaches are the oxidation-reduction reactions by which N<sub>2</sub>O is generated  
104 or consumed explicitly represented. Furthermore the effects of defoliation and surface litter on N<sub>2</sub>O  
105 emissions have not been considered in earlier process models.

106 Process models used to simulate N<sub>2</sub>O emissions must also accurately represent the key processes  
107 of C cycling that drive those of N cycling from which N<sub>2</sub>O is generated and consumed. These include  
108 gross and net primary productivity (GPP and NPP) which drive mineral N uptake and assimilation with  
109 plant growth. GPP and consequent plant growth also drive autotrophic respiration ( $R_a$ ), the below-  
110 ground component of which contributes to soil O<sub>2</sub> demand. NPP drives litterfall and root exudation,  
111 which in turn drive heterotrophic respiration ( $R_h$ ) that also contributes to litter and soil O<sub>2</sub> demand, and  
112 thereby to demand for alternative e<sup>-</sup> acceptors which drive N<sub>2</sub>O generation. Heterotrophic respiration  
113 also drives key N transformations such as mineralization/immobilization, thereby controlling availability  
114 of these alternative e<sup>-</sup> acceptors. Land use practices such as defoliation from grazing or harvesting, and

115 soil properties such as porosity and water retention, alter these key C cycling processes, and thereby  
116 N<sub>2</sub>O emissions. Therefore these emissions are best simulated by comprehensive ecosystem models.

117 In the mathematical model *ecosys*, the effects of weather and N amendments on  $T_s$ ,  $\theta$ , and  
118 mineral N, and hence on the demand for vs. supply of O<sub>2</sub>, NO<sub>3</sub><sup>-</sup>, NO<sub>2</sub><sup>-</sup> and N<sub>2</sub>O, and thereby on N<sub>2</sub>O  
119 emissions, are simulated by explicitly coupling the transport processes with the oxidation – reduction  
120 reactions by which these e<sup>-</sup> acceptors are known to be generated, transported and consumed in soils  
121 (Grant and Pattey, 1999, 2003, 2008; Grant et al., 2006; Metivier et al., 2009). The development of  
122 model algorithms for these processes was guided by two key principles:

- 123 (1) all algorithms in the model must represent physical, biochemical and biological processes  
124 studied in basic research programs (e.g. convective-diffusive transport, oxidation-reduction  
125 reactions) so that these algorithms can be parameterized independently of the model
- 126 (2) this parameterization must be conducted at spatial and temporal scales smaller than those of  
127 prediction (in this case seasonal N<sub>2</sub>O fluxes) so that site-specific effects on predicted values are  
128 not incorporated into the algorithms, limiting their robustness.

129 These principles are designed to avoid as much as possible the use of site- and model-specific  
130 algorithms that may lack application in sites and models other than those for which they were  
131 developed. Although models based on these principles appear complex, they can be better constrained  
132 than simpler models because they are parameterized from independent experiments. The resulting detail  
133 that application of these principles brings to the model enables better constrained tests of model output  
134 against more comprehensive and diverse site data than are possible with simpler models.

135 In an extension of earlier work with *ecosys*, we propose that temporal and spatial variation in  
136 N<sub>2</sub>O emissions from an intensively managed grassland can be largely explained from the modelled  
137 effects of N amendments (fertilizer, manure), plant management (e.g. harvest intensity and timing), soil  
138 properties (e.g. bulk density) and weather ( $T_s$ , precipitation events) on the demand for vs. supply of O<sub>2</sub>,  
139 NO<sub>3</sub><sup>-</sup>, NO<sub>2</sub><sup>-</sup> and N<sub>2</sub>O in surface litter and near-surface soil (0 – 2 cm). Testing this explanation requires  
140 frequent measurements to characterize the large temporal variation in N<sub>2</sub>O emissions found in managed  
141 ecosystems. Such measurements were recorded from 2004 to 2009 using automated chambers in

142 intensively managed grass-clover grassland at Oensingen, Switzerland, and used here to test our  
143 modelled explanation of these fluxes.

144

## 145 **MODEL DEVELOPMENT**

146

### 147 **General Overview**

148 The hypotheses for N<sub>2</sub>O oxidation-reduction reactions and their coupling with gas transport in  
149 *ecosys* are represented in Fig. 1 and described further below with reference to equations and definitions  
150 listed in Appendices A, C, D, E, H of the Supplement (indicated by square brackets in the text below,  
151 e.g. [H1] refers to Eq. 1 in Appendix H), as well as in earlier papers (Grant and Pattey, 1999, 2003,  
152 2008; Grant et al., 2006; Metivier et al., 2009). These hypotheses are part of a larger model of soil C, N  
153 and P transformations (Grant et al., 1993a,b), coupled to one of soil water, heat and solute transport in  
154 surface litter and soil layers, which are in turn components of the comprehensive ecosystem model  
155 *ecosys* (Grant, 2001).

156

### 157 **Mineralization and Immobilization of Ammonium by All Microbial Populations**

158 Heterotrophic microbial populations  $m$  (obligately aerobic bacteria, obligately aerobic fungi,  
159 facultatively anaerobic denitrifiers, anaerobic fermenters, acetotrophic methanogens, and obligately  
160 aerobic and anaerobic non-symbiotic diazotrophs) are associated with each organic substrate  $i$  ( $i =$   
161 animal manure, coarse woody plant residue, fine non-woody plant residue, particulate organic matter, or  
162 humus). Autotrophic microbial populations  $n$  (aerobic NH<sub>4</sub><sup>+</sup> and NO<sub>2</sub><sup>-</sup> oxidizers, hydrogenotrophic  
163 methanogens and methanotrophs) are associated with inorganic substrates. These populations grow with  
164 energy generated from coupled oxidation of reduced dissolved C (DOC) by heterotrophs, or of mineral  
165 N (NH<sub>4</sub><sup>+</sup> and NO<sub>2</sub><sup>-</sup>) by nitrifiers, and reduction of e- acceptors O<sub>2</sub> and NO<sub>x</sub>. These populations decay  
166 according to first-order rate constants with provision for internal recycling of limiting nutrients (N, P).  
167 During growth, each functional component  $j$  ( $j =$  nonstructural, labile, resistant) of these populations  
168 seeks to maintain a set C:N ratio by mineralizing NH<sub>4</sub><sup>+</sup> ([H1a]) from, or by immobilizing NH<sub>4</sub><sup>+</sup> ([H1b])  
169 or NO<sub>3</sub><sup>-</sup> ([H1c]) to, microbial nonstructural N. Nitrogen limitations during growth may cause C:N ratios  
170 to rise above set values, and greater recovery of microbial N from structural to nonstructural forms to

171 reduce N loss during decay, but at a cost to microbial function. These transformations control the  
 172 exchange of N between organic and inorganic states, and hence affect the availability of alternative  $e^-$   
 173 acceptors for nitrification and denitrification.

174

### 175 **Oxidation of DOC and Reduction of Oxygen by Heterotrophs**

176 Constraints on heterotrophic oxidation of DOC imposed by  $O_2$  uptake are solved in four steps:

- 177 1) DOC oxidation under non-limiting  $O_2$  is calculated from active biomass, DOC concentration, and an  
 178 Arrhenius function of  $T_s$  [H2],
- 179 2)  $O_2$  reduction to  $H_2O$  under non-limiting  $O_2$  ( $O_2$  demand) is calculated from 1) using a set respiratory  
 180 quotient [H3],
- 181 3)  $O_2$  reduction to  $H_2O$  under ambient  $O_2$  is calculated from radial  $O_2$  diffusion through water films of  
 182 thickness determined by soil water potential [H4a] coupled with active uptake at heterotroph surfaces  
 183 driven by 2) [H4b].  $O_2$  diffusion and active uptake is calculated for each heterotrophic population  
 184 associated with each organic substrate, allowing [H4] to calculate lower  $O_2$  concentrations at  
 185 microbial surfaces associated with more biologically active substrates (e.g. manure, litter). Localized  
 186 zones of low  $O_2$  concentration (hotspots) are thereby simulated when  $O_2$  uptake by any aerobic  
 187 population is constrained by  $O_2$  diffusion to that population.  $O_2$  uptake by each heterotrophic  
 188 population also accounts for competition for  $O_2$  uptake with other heterotrophs, nitrifiers, roots and  
 189 mycorrhizae, calculated from its  $O_2$  demand relative to those of other aerobic populations.
- 190 4) DOC oxidation to  $CO_2$  under ambient  $O_2$  is calculated from 2) and 3) [H5]. The energy yield of DOC  
 191 oxidation drives the uptake of additional DOC for construction of microbial biomass  $M_{i,h}$  according to  
 192 construction energy costs of each heterotrophic population [A21]. Energy costs of denitrifiers are  
 193 larger than those of obligately aerobic heterotrophs, placing denitrifiers at a competitive disadvantage  
 194 for growth and hence DOC oxidation that declines with greater use of  $e^-$  acceptors other than  $O_2$ .

195

### 196 **Oxidation of DOC and Reduction of Nitrate, Nitrite and Nitrous Oxide by Denitrifiers**

197 Constraints imposed by  $NO_3^-$  availability on DOC oxidation by denitrifiers are solved in five  
 198 steps:

- 199 1)  $NO_3^-$  reduction to  $NO_2^-$  under non-limiting  $NO_3^-$  is calculated from electrons demanded by DOC  
 200 oxidation to  $CO_2$  but met by  $O_2$  reduction to  $H_2O$  because of diffusion limitations to  $O_2$  supply, and  
 201 hence transferred to  $NO_3^-$  [H6],

- 202 2)  $\text{NO}_3^-$  reduction to  $\text{NO}_2^-$  under ambient  $\text{NO}_3^-$  is calculated from 1), accounting for relative  
 203 concentrations and affinities of  $\text{NO}_3^-$  and  $\text{NO}_2^-$  [H7],  
 204 3)  $\text{NO}_2^-$  reduction to  $\text{N}_2\text{O}$  under ambient  $\text{NO}_2^-$  is calculated from demand for electrons not met by  $\text{NO}_3^-$   
 205 reduction in 2), accounting for relative concentrations and affinities of  $\text{NO}_2^-$  and  $\text{N}_2\text{O}$  [H8],  
 206 4)  $\text{N}_2\text{O}$  reduction to  $\text{N}_2$  under ambient  $\text{N}_2\text{O}$  is calculated from demand for electrons not met by  $\text{NO}_2^-$   
 207 reduction in 3) [H9],  
 208 5) additional DOC oxidation to  $\text{CO}_2$  enabled by  $\text{NO}_x$  reduction in 2), 3) and 4) is added to that enabled  
 209 by  $\text{O}_2$  reduction from [H5], the energy yield of which drives additional DOC uptake for construction  
 210 of  $M_{i,n}$ . This additional uptake offsets the disadvantage incurred by the larger construction energy  
 211 costs of denitrifiers.

212

### 213 **Oxidation of Ammonia and Reduction of Oxygen by Nitrifiers**

214 Constraints on nitrifier oxidation of  $\text{NH}_3$  imposed by  $\text{O}_2$  uptake are solved in four steps:

- 215 1) substrate ( $\text{NH}_3$ ) oxidation under non-limiting  $\text{O}_2$  is calculated from active biomass,  $\text{NH}_3$  and  $\text{CO}_2$   
 216 concentrations, and an Arrhenius function of  $T_s$  [H11],  
 217 2)  $\text{O}_2$  reduction to  $\text{H}_2\text{O}$  under non-limiting  $\text{O}_2$  is calculated from 1) using set respiratory quotients [H12],  
 218 3)  $\text{O}_2$  reduction to  $\text{H}_2\text{O}$  under ambient  $\text{O}_2$  is calculated from radial  $\text{O}_2$  diffusion through water films of  
 219 thickness determined by soil water potential [H13a] coupled with active uptake at nitrifier surfaces  
 220 driven by 2) [H13b].  $\text{O}_2$  uptake by nitrifiers also accounts for competition for  $\text{O}_2$  uptake with  
 221 heterotrophic DOC oxidizers, roots and mycorrhizae,  
 222 4)  $\text{NH}_3$  oxidation to  $\text{NO}_2^-$  under ambient  $\text{O}_2$  is calculated from 2) and 3) [H14]. The energy yield of  $\text{NH}_3$   
 223 oxidation drives the fixation of  $\text{CO}_2$  for construction of microbial biomass  $M_{i,n}$  according to  
 224 construction energy costs of nitrifier populations.

225

### 226 **Oxidation of Nitrite and Reduction of Oxygen by Nitrifiers**

227 Constraints on nitrifier oxidation of  $\text{NO}_2^-$  to  $\text{NO}_3^-$  imposed by  $\text{O}_2$  uptake [H15 - H18] are solved  
 228 in the same way as are those of  $\text{NH}_3$  [H11 - H14]. The energy yield of  $\text{NO}_2^-$  oxidation drives the fixation  
 229 of  $\text{CO}_2$  for construction of microbial biomass  $M_{i,o}$  according to construction energy costs of each nitrifier  
 230 population.

231



### 232 **Oxidation of Ammonia and Reduction of Nitrite by Nitrifiers**

233 Constraints on nitrifier oxidation of  $\text{NH}_3$  imposed by  $\text{NO}_2^-$  availability are solved in three steps:

- 234 1)  $\text{NO}_2^-$  reduction to  $\text{N}_2\text{O}$  under non-limiting  $\text{NO}_2^-$  is calculated from electrons demanded by  $\text{NH}_3$   
 235 oxidation but not accepted for  $\text{O}_2$  reduction to  $\text{H}_2\text{O}$  because of diffusion limitations to  $\text{O}_2$  supply, and  
 236 hence transferred to  $\text{NO}_2^-$  [H19],  
 237 2)  $\text{NO}_2^-$  reduction to  $\text{N}_2\text{O}$  under ambient  $\text{NO}_2^-$  and  $\text{CO}_2$  is calculated from 1) [H20], competing for  $\text{NO}_2^-$   
 238 with denitrifiers [H8] and nitrifiers [H18],  
 239 3) additional  $\text{NH}_3$  oxidation to  $\text{NO}_2^-$  enabled by  $\text{NO}_2^-$  reduction in 2) [H21] is added to that enabled by  
 240  $\text{O}_2$  reduction from [H14]. The energy yield from this oxidation drives the fixation of additional  $\text{CO}_2$   
 241 for construction of  $M_{i,n}$ .

### 243 **Uptake of Ammonium and Reduction of Oxygen by Roots and Mycorrhizae**

- 244 1)  $\text{NH}_4^+$  uptake by roots and mycorrhizae under non-limiting  $\text{O}_2$  is calculated from mass flow and radial  
 245 diffusion between adjacent roots and mycorrhizae [C23a] coupled with active uptake at root and  
 246 mycorrhizal surfaces [C23b]. Active uptake is subject to inhibition by root nonstructural N:C ratios  
 247 [C23g] where nonstructural N is the active uptake product, and nonstructural C is the  $\text{CO}_2$  fixation  
 248 product transferred to roots and mycorrhizae from the canopy.  
 249 2)  $\text{O}_2$  reduction to  $\text{H}_2\text{O}$  is calculated from 1) plus oxidation of root and mycorrhizal nonstructural C  
 250 under non-limiting  $\text{O}_2$  using a set respiratory quotient [C14e],  
 251 3)  $\text{O}_2$  reduction to  $\text{H}_2\text{O}$  under ambient  $\text{O}_2$  is calculated from mass flow and radial diffusion between  
 252 adjacent roots and mycorrhizae [C14d] coupled with active uptake at root and mycorrhizal surfaces  
 253 driven by 2) [C14c].  $\text{O}_2$  uptake by roots and mycorrhizae also accounts for competition with  $\text{O}_2$   
 254 uptake by heterotrophic DOC oxidizers, and autotrophic nitrifiers, calculated from their  $\text{O}_2$  demands  
 255 relative to those of other populations.  
 256 4) oxidation of root and mycorrhizal nonstructural C to  $\text{CO}_2$  under ambient  $\text{O}_2$  is calculated from 2) and  
 257 3) [C14b],  
 258 5)  $\text{NH}_4^+$  uptake by roots and mycorrhizae under ambient  $\text{O}_2$  is calculated from 1), 2), 3) and 4) [C23b].  
 259

### 260 **Cation Exchange and Ion Pairing of Ammonium**

261 A Gapon selectivity coefficient is used to solve cation exchange of  $\text{NH}_4^+$  vs.  $\text{Ca}^{2+}$  [E10] as  
262 affected by other cations [E11] – [E15] and CEC [E16]. A solubility product is used to equilibrate  
263 soluble  $\text{NH}_4^+$  and  $\text{NH}_3$  [E24] as affected by pH [E25] and other solutes [E26 – E57].  
264

### 265 **Soil Transport and Surface - Atmosphere Exchange of Gaseous Substrates and Products**

266 Exchange of all modelled gases  $\gamma$  ( $\gamma = \text{O}_2, \text{CO}_2, \text{CH}_4, \text{N}_2, \text{N}_2\text{O}, \text{NH}_3$  and  $\text{H}_2$ ) between aqueous  
267 and gaseous states is driven by disequilibrium between aqueous and gaseous concentrations according to  
268 a  $T_s$ -dependent solubility coefficient, constrained by a transfer coefficient based on air-water interfacial  
269 area that depends on air-filled porosity [D14 – D15] (Fig. 1). These gases undergo convective-dispersive  
270 transport through soil in gaseous [D16] and aqueous [D19] states driven by soil water flux and by gas  
271 concentration gradients. Dispersive transport is controlled by gaseous diffusion [D17] and aqueous  
272 dispersion [D20] coefficients calculated from gas- and water-filled porosity. Exchange of all gases  
273 between the atmosphere and both gaseous and aqueous states at the soil surface are driven by  
274 atmosphere - surface gas concentration differences and by boundary layer conductance above the soil  
275 surface, calculated from wind speed and from structure of vegetation and surface litter [D15].  
276

## 277 **FIELD EXPERIMENT**

278

### 279 **Site description**

280 The Oensingen field site is located in the central Swiss lowlands ( $7^\circ 44'E, 47^\circ 17'N$ ) at an altitude  
281 of 450 m. The climate is temperate with an average annual rainfall of about 1100 mm and a mean air  
282 temperature of  $9.5^\circ\text{C}$ . The soil is classified as a Eutri-Stagnic Cambisol developed on clayey alluvial  
283 deposits, key properties of which are given in Table 1. Prior to the experiment, the field site was  
284 managed as a ley-arable rotation. In December 2000, the field was ploughed and left in fallow until  
285 11 May 2001. The field was then sown with a grass-clover mixture typical for permanent grassland  
286 under intensive management. The field was ploughed again on 19 December 2007, left in fallow until  
287 5 May 2008, when it was tilled and re-sown with the same grass-clover mix as in 2001. The period  
288 of study extended from sowing in 2001 to the end of 2009, during which the field was cut between  
289 three and five times per year and harvested as hay, silage or fresh grass, fertilized two to three times  
290 per year with manure as liquid cattle slurry and two to three times per year with mineral fertilizer as

291 ammonium nitrate ( $\text{NH}_4\text{NO}_3$ ) pellets, for an average annual N application of  $23 \text{ g N m}^{-2}$ . All key  
292 management operations during this period are summarized in Table 2.

293

### 294 **Soil, plant and meteorological measurements**

295 Soil  $\theta$  and  $T_s$  were recorded continuously using TDR (Time Domain Reflectometry, ThetaProbe  
296 ML2x, Delta-T Devices, Cambridge, UK) and thermocouples at 5, 10, 30 and 50 cm for  $\theta$  and at 2, 5,  
297 10, 30 and 50 cm for  $T_s$ . Leaf area index (LAI) was measured weekly with an optical leaf area meter  
298 (LI-2000, Li-Cor, Lincoln, NB, USA). Plants were collected every 2 to 4 weeks and the samples were dried  
299 for 48 h at  $80^\circ\text{C}$ , weighed and analyzed for C, N, P and K by using an elemental analyzer. Hourly  
300 climatic data were recorded continuously with an automated meteorological station, including air  
301 temperature ( $^\circ\text{C}$ ), rainfall (mm), relative humidity (%), global radiation ( $\text{W m}^{-2}$ ) and windspeed ( $\text{m}$   
302  $\text{s}^{-1}$ ).

303

### 304 **Nitrous oxide flux measurements**

305  $\text{N}_2\text{O}$  fluxes were measured with a fully automated system consisting of up to eight stainless steel  
306 chambers ( $30 \text{ cm} \times 30 \text{ cm} \times 25 \text{ cm}$ ) (Flechard et al., 2005, Felber et al., 2014) fixed on PVC frames  
307 permanently inserted 10-cm deep into the soil. The positions of the chambers were changed about every  
308 two months. During measurements, the lids of the chambers were sequentially closed for 15 min. every  
309 2 hours to allow  $\text{N}_2\text{O}$  accumulation in the chamber headspace. During closure the chamber atmosphere  
310 was recirculated at a rate of  $1000 \text{ ml min}^{-1}$  through polyamide tube lines (4-mm ID) to analytical  
311 instruments installed in a temperature-controlled field cabin adjacent to the field plots (10 m) and then  
312 back to the chamber headspace. Until autumn 2006 concentrations of  $\text{N}_2\text{O}$ ,  $\text{CO}_2$  and  $\text{H}_2\text{O}$  in the head  
313 space were measured once per minute with an INNOVA 1312 photoacoustic multi-gas analyzer  
314 (INNOVA Air Tech Instruments, Ballerup, Denmark; [www.innova.dk](http://www.innova.dk)). Interferences in the  
315 measurements caused by overlaps in the absorption spectra of the different gases and by temperature  
316 effects were corrected with a calibration algorithm described in detail by Flechard et al (2005). In  
317 autumn 2006 the system was changed to the gas filter correlation technique for  $\text{N}_2\text{O}$  (Model 46C,  
318 Thermo 279 Environmental Instruments Inc., Sunnyvale, CA, USA). This system was calibrated every 8  
319 hours using certified standard gas mixtures (Messer Schweiz AG, Lenzburg, Switzerland) (Felber et al.  
320 2014).

321

322 These measurements were used to calculate N<sub>2</sub>O fluxes from the rate of change in concentration  
323 by using a linear or non-linear approach determined by the HMR R-package (Pedersen et al., 2010). The  
324 first three of the fifteen 1-min. measurements were omitted from the flux calculation to exclude gas  
325 exchange during closing that did not result from changes in emission/production in the soil. This  
326 procedure caused a mean increase of about 30% in the fluxes compared to values published in Fléchar  
327 et al. (2005) and Ammann et al. (2009), which were evaluated using linear regression. Fluxes from all  
328 chambers were averaged over 4-hourly intervals and resulting values attributed to the mid-points of the  
329 intervals. Standard errors of these averages were calculated from all fluxes measured during each  
330 interval, and thus included both spatial and temporal variation. The fluxes measured from 2002 to 2003  
331 were summarized in Fléchar et al. (2005). Those from 2004 to 2007 were re-evaluated from values  
332 described in Ammann et al. (2009). Those from 2008 and 2009 were reprocessed from the EU-Project  
333 NitroEurope-IP database using the HMR algorithm.

334

### 335 **CO<sub>2</sub> and Energy Flux Measurements**

336 CO<sub>2</sub> and energy fluxes were measured by an eddy covariance (EC) system consisting of three-  
337 axis sonic anemometers (models R2 and HS, Gill instruments, Lymington, UK) and an open-path  
338 infrared CO<sub>2</sub>/H<sub>2</sub>O gas analyzer (model LI-7500, Li-Cor, Lincoln, USA). The EC system used in this  
339 study is described in Ammann et al. (2007). The EC tower was located in the centre of the field (52m  
340 x 146m), whereas the chambers were located in the south east corner. For most meteorological  
341 conditions, the chambers were not within the footprint of the EC towers, although for the main wind  
342 directions 80% or more of the footprint was within the field (Neftel et al. 2008). The management of  
343 the entire field was uniform throughout the experiment.

344

## 345 **MODEL EXPERIMENT**

346

347 *Ecosys* was initialized with the biological properties of plant functional types (PFTs)  
348 representing the ryegrass and clover planted at Oensingen. These properties were identical to those in an  
349 earlier study (Grant et al., 2012) except for a perennial rather than annual growth habit. These PFTs  
350 competed for common resources of radiation, water and nutrients, based on their vertical distributions of  
351 leaf area and root length driven by uptake and allocation of C, N and P in each PFT. *Ecosys* was also  
352 initialized with the physical and chemical properties of the Eutri-Stagnic Cambisol at Oensingen (Table

353 1). The model was then run from model dates 1 Jan. 1931 to 31 Dec. 2000 under repeating sequences of  
354 land management practices and continuous hourly weather data (radiation,  $T_a$ , RH, wind speed and  
355 precipitation) recorded at Oensingen from 1 Jan. 2001 to 31 Dec. 2007 (i.e. 10 cycles of 7 years). This  
356 run was long enough for C, N and energy cycles in the model to attain equilibrium under the Oensingen  
357 site conditions well before the end of the spinup run. The modelled site was plowed on 19 Dec. 2000,  
358 terminating all PFTs.

359 The model run was then continued from model dates 1 Jan. 2001 to 31 Dec. 2009 under  
360 continuous hourly weather data recorded at Oensingen from 1 Jan. 2001 to 31 Dec. 2009 with the  
361 same PFTs and land management practices as those at the field site listed in Table 2. For each manure  
362 application in the model, an irrigation of 4 mm was added to account for the water in the slurry. For  
363 each harvest in the model, the fraction of canopy LAI to be cut (usually 0.85 – 0.95) was calculated  
364 from measurements of LAI before and after the corresponding harvest in the field. In *ecosys*, leaves of  
365 each PFT are aggregated into a common canopy which is dynamically resolved into a selected  
366 number of layers (10 in this case) of equal LAI for calculating irradiance interception. The leaf  
367 fraction to be cut was removed from successive leaf layers from the top of the combined canopy  
368 downwards until the cumulative removal attained the set fraction, so that the LAI cut from each PFT  
369 depended on the leaf area of the PFT in these layers. Of the phytomass cut with the LAI, 0.76 was  
370 removed as harvest and the remainder was added to surface litter, as determined in the intensively  
371 managed grassland at Oensingen by Amman et al. (2009). N<sub>2</sub>O emissions modelled from 2004  
372 through 2009 were compared with those measured by the automated chambers by regressing log-  
373 transformed 4-hour averages of modelled on measured values during each year of the study. These  
374 comparisons were supported by ones with thermistor and TDR measurements of  $T_s$ ,  $\theta$ , and with EC  
375 measurements of CO<sub>2</sub> and energy exchange.

376

377

### Model Sensitivity Studies

378 Modelled N<sub>2</sub>O emissions may be affected by three general sources of uncertainty in model  
379 inputs: land management practices, soil properties and model parameters. To examine the possible  
380 effects of some different land management practices on N<sub>2</sub>O emissions, the model run from 2001 to  
381 2009 (field) was repeated with (1) increased harvest intensity in which canopy LAI remaining after  
382 each harvest was reduced to one-half of those in the first run (1/2), and (2) increased harvest intensity  
383 with each harvest delayed by 5 days (1/2 + 5d). These alternative practices caused canopy regrowth

384 and hence N uptake to be slower during emission events following subsequent manure and fertilizer  
385 applications.

386

387 To examine the possible effects of spatial variability in soil properties on N<sub>2</sub>O emissions, the  
388 model run from 2001 to 2009 (field) was repeated with bulk density (BD) of the upper 3 cm in the soil  
389 profile (Table 1) increased by 5% or 10%. These larger BDs reduced soil porosity in the upper 3 cm  
390 of the soil, thereby slowing gas exchange with the atmosphere, particularly when the soil was wet  
391 (Fig. 1). All other soil properties used in the model remained unchanged (Table 1).

392

393 To examine an effect of uncertainty in model parameterization, the model run from 2001 to  
394 2009 (field) was repeated with the values of two key parameters governing N<sub>2</sub>O emissions, the  
395 Michaelis-Menten constants for reduction of O<sub>2</sub> ( $K_{O_2}$  in [H4]) or of NO<sub>3</sub><sup>-</sup> and NO<sub>2</sub><sup>-</sup> ( $K_{NO_x}$  in [H7],  
396 [H8] and [H20]), halved or doubled from those used in the model. Halving or doubling  $K_{O_2}$  hastened  
397 or slowed the reduction of O<sub>2</sub> by nitrifiers and denitrifiers and hence slowed or hastened the transfer  
398 of electrons to reduce NO<sub>2</sub><sup>-</sup> and NO<sub>3</sub><sup>-</sup> during nitrification and denitrification. Halving or doubling  
399  $K_{NO_x}$  hastened or slowed the reduction of NO<sub>2</sub><sup>-</sup> by nitrifiers and of NO<sub>3</sub><sup>-</sup> and NO<sub>2</sub><sup>-</sup> by denitrifiers All  
400 other parameters in the model remained unchanged.

401

402

403

## RESULTS

404

### LAI Modelled vs. Measured from 2002 to 2009

406 Accurate modelling of ecosystem C cycling and hence N<sub>2</sub>O emissions requires accurate  
407 modelling of plant growth as determined by land management practices. LAI modelled and measured  
408 from 2002 to 2009 rose rapidly from low values remaining in spring and after each harvest (Table 1)  
409 to 4 – 6 m<sup>2</sup> m<sup>-2</sup> before the next harvest, except during 2003 (Fig. 2). Regrowth of LAI in *ecosys* was  
410 driven by plant nonstructural C, N and P pools replenished from storage reserves remobilized after  
411 harvests, and from products of current C, N and P uptake, those of C being governed by irradiance  
412 interception calculated from regrowing LAI. Regrowth in the model was less rapid than that measured  
413 in 2009 (Fig. 2) because more frequent cutting forced more frequent replenishment of plant  
414 nonstructural C, N and P pools which gradually depleted storage reserves and hence slowed

415 subsequent regrowth. Hence rates of regrowth modelled after harvests were affected by harvest timing  
416 and intensity, as represented by the fractions of LAI removed at harvest.

### 417 418 **N<sub>2</sub>O Fluxes Modelled vs. Measured from 2004 to 2009**

419 During peak emissions, standard deviations of N<sub>2</sub>O fluxes measured within each 4-hourly  
420 interval were found to be as much as 85% relative to mean values. These deviations were largely  
421 attributed to small-scale spatial variation in land management (manure and fertilizer application,  
422 surface litter from harvesting) and in soil properties (bulk density, water retention), which was not  
423 represented in the model run, rather than to temporal variation in environmental conditions ( $\theta$ ,  $T_s$ )  
424 which was represented in the model run. Therefore only a limited fraction of variation in the  
425 measured values was amenable to correlation with modelled values. Consequently slopes and  
426 coefficients of determination ( $R^2$ ) from regressions of modelled on measured log-transformed fluxes  
427 varied from 0.5 to 1.0 and from 0.1 to 0.5 respectively, while intercepts remained close to zero (Table  
428 3). However ratios of mean squares for regression vs. error (F) were highly significant ( $P < 0.001$ ) in  
429 all years of the study, indicating some agreement in the timing and magnitude of modelled and  
430 measured emission events. Improved agreement would require that more detailed information about  
431 land management and soil properties at each chamber site be provided to the model.

### 432 433 **Daily-Aggregated N<sub>2</sub>O Fluxes Modelled vs. Measured from 2004 to 2009**

434 Daily aggregations of both measured and modelled N<sub>2</sub>O emissions indicated that emission  
435 events during the study period were confined to intervals of no longer than 5 days when precipitation  
436 followed manure or fertilizer applications (Fig. 3). Outside of these intervals emissions remained very  
437 small except for a period of emissions modelled, but not measured, after manure application in  
438 autumn 2006 (Fig. 3c) and measured, but not modelled, before fertilizer application in spring 2008  
439 (Fig. 3e).

440  
441 The largest emissions followed manure applications in July and August, but their magnitudes  
442 did not vary with the amount of manure N applied. For example, emissions during an event in August  
443 2009 (244 vs. 185 mg N m<sup>-2</sup> measured vs. modelled in Fig. 3f) were greater than those during an  
444 event in July 2007 (86 vs. 112 mg N m<sup>-2</sup> measured vs. modelled in Fig. 3d) which in turn were greater  
445 than those during an event in July 2005 (54 vs. 96 mg N m<sup>-2</sup> measured vs. modelled in Fig.2b).

446 However manure N application preceding the event in August 2009 ( $4.5 \text{ g N m}^{-2}$ ) was less than that in  
447 July 2007 ( $6.7 \text{ g N m}^{-2}$ ) which in turn was less than that in July 2005 ( $8.5 \text{ g N m}^{-2}$ ) (Table 2), so that  
448 smaller applications were followed by greater emissions, precluding a simple emission factor for  
449 manure N application.

450

451 The magnitude of emission events following fertilizer application also varied. For example,  
452 emissions during an event in late August 2007 ( $105 \text{ vs. } 82 \text{ mg N m}^{-2}$  measured vs. modelled in Fig.  
453 3d) were greater than those during events in September 2004 ( $24 \text{ vs. } 2 \text{ mg N m}^{-2}$  measured vs.  
454 modelled in Fig 2a) and 2005 ( $6 \text{ vs. } 11 \text{ mg N m}^{-2}$  measured vs. modelled in Fig. 3b), although the  
455 fertilizer N applications of  $3.0 \text{ g N m}^{-2}$  preceding each event were the same (Table 2). These  
456 differences in emissions indicated important differences in ecological controls imposed by  
457 environmental conditions ( $\theta$  and  $T_s$ ) and plant management during each event.

458

459 The standard deviations of  $\sim 85\%$  relative to the mean values of fluxes measured within each 4-  
460 hourly interval during emission events was used to estimate an uncertainty in daily-aggregated fluxes  
461 of *ca.* 30%. Uncertainty in daily fluxes measured during emission events was smaller than the several-  
462 fold differences among the events indicating that the magnitude of these events likely differed  
463 significantly.

464

#### 465 **Relationships between N<sub>2</sub>O Fluxes and Environmental Conditions during Selected Emission** 466 **Events**

467 Environmental conditions measured and modelled from harvest to the end of the two largest  
468 emission events following manure applications in July 2007 (Fig. 3d) and August 2009 (Fig. 3f) were  
469 examined in greater detail to investigate relationships among near-surface  $T_s$ ,  $\theta$ , aqueous gas  
470 concentrations, and surface fluxes of energy, CO<sub>2</sub> and N<sub>2</sub>O (Figs. 4 and 5). In July 2007, several small  
471 precipitation events wetted and cooled the soil between harvesting on DOY 187 and manure  
472 application on DOY 194 (Fig. 4a,b). The soil then dried during several days without precipitation and  
473 warmed with reduced shading from defoliation (Fig. 2) until DOY 200, after which the soil wetted  
474 with further precipitation and cooled with increased shading from plant regrowth (Fig. 4a,b). The  
475 higher  $\theta$  measured during this period (Fig. 4b) may have been caused by difficulties in maintaining  
476 calibration of the TDR probes over long periods in the high-clay soil at Oensingen (Table 1). This



477 higher  $\theta$  was not likely caused by overestimated evapotranspiration because modelled LE fluxes,  
478 reduced by low LAI after harvesting but increasing with subsequent regrowth, were close to those  
479 measured (Fig. 4c), suggesting that total water uptake was accurately modelled. Comparison of  
480 modelled and measured  $\theta$  was further complicated by soil cracking which altered infiltration at low  $\theta$ .  
481 The effects of  $\theta$ -dependent macroporosity on preferential flow are explicitly modelled in *ecosys*, but  
482 have not yet been tested in detail.

483

484 CO<sub>2</sub> influxes were also reduced by low LAI after cutting, but recovered to pre-cut levels by the  
485 end of the emission event (Fig. 4d), driving rapid regrowth of LAI (Fig. 2). Large CO<sub>2</sub> effluxes  
486 measured and modelled after manure application indicated rapid  $R_h$  and hence O<sub>2</sub> demand that  
487 persisted for several days.. Influxes measured in the field were reduced from those in the model for  
488 several days after manure application, suggesting temporary interference of CO<sub>2</sub> fixation by the  
489 manure application which was not accounted for in the model.

490

491 Litterfall from plant growth [C18, C19] and cutting, as well as from manure application caused  
492 a litter layer of 1 – 2 cm to develop on the soil surface in the model. During the N<sub>2</sub>O emission event  
493 from DOY 200 to DOY 205 in 2007 (Fig. 3d), several precipitation events (Fig. 4a) wetted the  
494 modelled surface litter and near-surface soil (layers 1 and 2 in Table 1) (Fig. 4e) without increasing  $\theta$   
495 at 5 cm (Fig. 4b). This surface wetting slowed gas exchange with the atmosphere, sharply reducing  
496 aqueous O<sub>2</sub> concentrations [O<sub>2(s)</sub>] (Fig. 4f) and thereby raising aqueous N<sub>2</sub>O concentrations [N<sub>2</sub>O<sub>(s)</sub>]  
497 (Fig. 4g). Between precipitation events, drying of the surface litter and near-surface soil in the model  
498 allowed recovery of [O<sub>2(s)</sub>] and forced declines in [N<sub>2</sub>O<sub>(s)</sub>]. These rises and declines in [N<sub>2</sub>O<sub>(s)</sub>] drove  
499 rises and declines in N<sub>2</sub>O emissions that tracked those measured in the chambers (Fig. 4h). These  
500 emissions rose immediately with the onset of precipitation on DOY 200 (Fig. 4a) before wetting  
501 occurred at 5 cm (Fig. 4b), indicating that emissions were driven by surface wetting (Fig. 4e)  
502 combined with rapid O<sub>2</sub> demand (Fig. 4d). The net generation of N<sub>2</sub>O modelled in each soil zone,  
503 calculated from [H8] + [H20] – [H9], indicated that 0.21 of surface emissions originated in the surface  
504 litter and the remainder in the 0 – 1 cm soil layer as indicated by higher [N<sub>2</sub>O<sub>(s)</sub>] (Fig. 4g), while the  
505 deeper soil layers were a very small net sink of N<sub>2</sub>O. Rises and declines in [N<sub>2</sub>O<sub>(s)</sub>] also drove rises  
506 and declines in N<sub>2</sub> emissions that persisted until DOY 205, after which more rapid mineral N uptake

507 with recovering plant growth, driven by rising LAI (Fig. 2) and hence CO<sub>2</sub> influxes (Fig. 4d), caused  
508 both emissions to return to background levels (Fig. 4h).

509

510 In 2009, a period of low precipitation with soil drying and warming occurred between  
511 harvesting in late July and manure application on DOY 218 in early August, followed by heavy  
512 precipitation with soil wetting and cooling on DOY 220 (Fig. 5a,b). LE effluxes and CO<sub>2</sub> influxes  
513 declined sharply with LAI after cutting, and did not recover to pre-cut levels by the end of the  
514 subsequent emission event on DOY 224 (Fig. 5c,d), indicating a slow recovery of plant growth.  
515 Slurry application caused brief surface wetting on DOY 218 (Fig. 5e) and heavy precipitation on  
516 DOY 220 caused prolonged soil wetting at the surface (Fig. 5e) and at 5 cm (Fig. 5b). Wetting caused  
517 declines in [O<sub>2(s)</sub>] (Fig. 5f) and thereby rises in [N<sub>2</sub>O<sub>(s)</sub>] (Fig. 5g) that were sustained over 3 days.  
518 These rises drove particularly rapid N<sub>2</sub>O emissions in the model which were consistent in magnitude  
519 with those measured in the chambers (Fig. 5h). Diurnal variation modelled with soil warming and  
520 cooling (Fig. 5a) was not apparent in the measurements, although modelled values remained within  
521 the large uncertainty of the measured values during the emission event. These large emissions were  
522 enabled in the model by slow plant uptake of manure N (Table 2) caused by the slow recovery of  
523 plant CO<sub>2</sub> uptake and hence growth after cutting (Fig. 5d). The rises in [N<sub>2</sub>O<sub>(s)</sub>] also drove rises in  
524 modelled N<sub>2</sub> emissions (Fig. 5h). Emissions declined with surface litter drying on DOY 223 (Fig. 5e)  
525 which allowed surface [O<sub>2(s)</sub>] to rise (Fig. 5f) and [N<sub>2</sub>O<sub>(s)</sub>] to fall (Fig. 5g) while  $\theta$  at 5 cm remained  
526 high (Fig. 5b), again indicating that N<sub>2</sub>O emissions were largely determined by ecological controls in  
527 the surface litter and soil. The net generation of N<sub>2</sub>O modelled in each soil zone indicated that 0.48 of  
528 surface emissions originated in the surface litter, 0.48 in the 0 – 1 cm soil layer and 0.05 in the 1 – 3  
529 cm soil layer, while the deeper soil layers were a very small net sink of N<sub>2</sub>O, as indicated by near-  
530 surface gradients of [N<sub>2</sub>O<sub>(s)</sub>] (Fig. 5g).

531

532 Greater N<sub>2</sub>O emissions were modelled and measured during the event in August 2009 than in  
533 July 2007 (Fig. 5h vs. Fig. 4h), in spite of smaller N addition (Fig. 3f vs. Fig. 3d; Table 2) and similar  
534  $\theta$  and  $T_s$  modelled and measured at 5 cm (Fig. 5a,b vs. Fig. 4a,b). These greater emissions were  
535 attributed in the model to (1) earlier and heavier precipitation after manure application (2 days after  
536 application in Fig. 5a vs. 6 days in Fig. 4a), and (2) slower recovery of CO<sub>2</sub> fixation after defoliation,  
537 indicated by slower rises in diurnal amplitude of CO<sub>2</sub> fluxes (Fig. 5d vs. Fig. 4d). Heavier

538 precipitation in 2009 vs. 2007 drove sustained vs. intermittent surface and near-surface wetting (Fig.  
 539 5e vs. Fig. 4e) and hence sustained vs. intermittent declines in  $[O_{2(s)}]$  and rises in  $[N_2O_{(s)}]$  (Fig. 5f,g  
 540 vs. Fig. 4f,g). Slower recovery of  $CO_2$  fixation after cutting in 2009 vs. 2007 slowed removal of added  
 541  $NH_4^+$  and  $NO_3^-$  from soil. This slower removal, combined with the shorter period between manure  
 542 application and precipitation, left larger  $NO_3^-$  concentrations ( $[NO_3^-]$ ) in litter and surface soil to drive  
 543  $N_2O$  production following precipitation [H7]. These model findings indicated the importance to  $N_2O$   
 544 emissions of surface and near-surface  $\theta$  after precipitation, and of plant management (intensity and  
 545 timing of defoliation in relation to N application) and its effect on subsequent plant  $CO_2$  fixation and  
 546 N uptake.

547

### 548 **Effects of Intensity and Timing of Defoliation on $N_2O$ Emission Events**

549 Increasing harvest intensity and delaying harvest dates slowed LAI regrowth modelled after  
 550 harvests (Fig. 6). The effects of this slowing on  $N_2O$  emissions during selected events modelled after  
 551 subsequent fertilizer and manure applications were examined under diverse  $\theta$  and  $T_s$  (Figs. 7, 8).  
 552 Following manure application on DOY 194 in 2006 (Table 2), slower LAI regrowth from increasing  
 553 and delaying defoliation slowed the recovery of  $CO_2$  fixation (Fig. 7a) and of  $NH_4^+$  uptake (Fig. 7b),  
 554 allowing more nitrification of manure N and hence greater surface  $[NO_3^-]$  (Fig. 7c). Slower LAI  
 555 regrowth (Fig. 6) also reduced shading and ET, raising  $T_s$  (Fig. 7d) and  $\theta$  (Fig. 7e).  $N_2O$  emissions  
 556 modelled under field management remained small because of soil drying, in spite of high  $T_s$ ,  
 557 consistent with measurements (Fig. 3c, Fig. 7f). Increases in emissions modelled with slower LAI  
 558 regrowth, particularly from delayed harvesting (Fig. 7f), were attributed to slower N uptake (Fig. 7b)  
 559 and hence larger  $[NO_3^-]$  in litter and surface soil (Fig. 7c), and to warmer and wetter soil (Fig. 7d,e)  
 560 which increased  $O_2$  demand while reducing  $O_2$  supply.

561

562 Following a similar manure application on DOY 194 in 2007 (Table 2; Fig. 6), slower LAI  
 563 regrowth from increasing and delaying defoliation also caused reductions in  $CO_2$  fixation (Fig. 7g),  
 564 which slowed  $NH_4^+$  and  $NO_3^-$  uptake (Fig. 7h), allowing more nitrification of manure N and hence  
 565 greater  $[NO_3^-]$  (Fig. 7i). Lower LAI also caused increases in  $T_s$  (Fig. 7j) and  $\theta$  (Fig. 7k). Emissions  
 566 modelled and measured under field management in 2007 (Fig. 7l) were greater than those in 2006  
 567 (Fig. 7f), in spite of lower  $T_s$  (Fig. 7j vs. Fig. 7d), because near-surface wetting from several  
 568 precipitation events (Fig. 4a,e) reduced  $[O_{2(s)}]$  and increased  $[N_2O_{(s)}]$  (Fig. 4f,g). Emissions modelled

569 with increased and delayed harvesting rose from those with field harvesting as the emission event  
 570 progressed (Fig. 7l) because elevated  $[\text{NO}_3^-]$  from the manure application persisted longer during the  
 571 event (Fig. 7i).

572

573 Following fertilizer application on DOY 259 in 2005 (Table 2), modelled and measured  
 574 emissions remained small after soil wetting (Fig. 8f) because lower  $T_s$  (Fig. 8d) slowed soil  
 575 respiration after wetting, manifested as smaller measured and modelled  $\text{CO}_2$  effluxes (Fig. 8a), and so  
 576 slowed demand for  $e^-$  acceptors. Under these conditions, increasing and delaying defoliation had little  
 577 effect on modelled  $\text{N}_2\text{O}$  emissions (Fig. 8f), while  $\text{CO}_2$  fixation (Fig. 8a) and N uptake (Fig. 8b) were  
 578 only slightly reduced and surface  $\text{NO}_3^-$  only slightly increased (Fig. 8c). Following the same fertilizer  
 579 application on DOY 240 in 2007, modelled and measured emissions were greater than those in 2005  
 580 (Fig. 8l) because soils were warmer (Fig. 8j) with more rapid respiration (Fig. 8g), and because  
 581 fertilizer application and subsequent wetting occurred sooner after cutting (Table 2). Consequently  
 582 recovery of  $\text{CO}_2$  fixation was less advanced (Fig. 8g), reducing cumulative N uptake (Fig. 8h) and  
 583 leaving larger  $[\text{NO}_3^-]$  to drive  $\text{N}_2\text{O}$  generation during the event (Fig. 8h). However reducing LAI  
 584 remaining after each harvest did not raise  $\text{N}_2\text{O}$  emissions after this application (Fig. 8l), because  
 585 slower LAI regrowth from earlier harvests had reduced primary productivity and consequently  
 586 litterfall and hence the mass of the surface litter from which much of the emitted  $\text{N}_2\text{O}$  was generated.  
 587 Consequently more intense harvests could cause surface litter later in the year to decline to levels at  
 588 which  $\text{N}_2\text{O}$  generation modelled in the litter was reduced.

589

### 590 **Annual Productivity, $\text{N}_2\text{O}$ Emissions and the Effects of Defoliation Intensity and Timing**

591 In the model, plant management practices affected LAI regrowth (Fig. 6),  $\text{CO}_2$  fixation, N  
 592 uptake, and hence soil  $[\text{NO}_3^-]$  and  $\text{N}_2\text{O}$  emissions (Figs. 7,8). These effects were summarized at an  
 593 annual time scale in Table 4. Modelled and EC-derived gross primary productivity (GPP) remained  
 594 close to  $2000 \text{ g C m}^{-2} \text{ y}^{-1}$  during most years except with low precipitation in 2003 and replanting in  
 595 2008, indicating a highly productive ecosystem with rapid C cycling and hence rapid demand for  $e^-$   
 596 acceptors (Table 4). Larger modelled vs. measured GPP caused larger modelled vs. measured NEP in  
 597 2003, 2005 and 2007. Harvest removals in the model varied with NEP except during replanting in  
 598 2008, but tended to exceed those recorded in the field, particularly with low EC-derived NEP in 2005  
 599 and 2006. Modelled values were determined in part by the assumed constant harvest efficiency of

600 0.76. Including C inputs from manure applications, modelled and estimated net biome productivity  
601 (NBP) were positive except during replanting in 2008, indicating that this intensively managed  
602 grassland was a C sink unless replanted. Average annual NBP modelled vs. measured from 2002 to  
603 2009 was 30 vs. 58 g C m<sup>-2</sup>, with the lower modelled value attributed to greater modelled harvest  
604 removals, particularly in 2006.

605

606 Slower LAI regrowth from increasing and delaying defoliation (Fig. 6) reduced modelled GPP,  
607  $R_e$  and hence NEP by 5 - 10% during years with greater productivity. However increasing and  
608 delaying defoliation did not much affect harvest removals because reduced NEP was offset by greater  
609 harvest intensity, so that NBP was reduced except with replanting in 2008.

610

611 Annual N<sub>2</sub>O emissions were estimated from chamber measurements for each year of the study  
612 by scaling the mean measured fluxes to annual values. These values are presented in Table 4 as upper  
613 boundaries for annual emissions because flux measurements from which means were calculated were  
614 more frequent during emission events. A lower boundary for annual emissions was also estimated in  
615 Table 4 by replacing missing flux measurements with zero. Average lower and upper boundaries for  
616 annual emissions estimated from 2002 to 2009 were 0.220 and 0.355 g N m<sup>-2</sup> respectively vs. an  
617 average annual emission in the model of 0.260 g N m<sup>-2</sup> (Table 4). Modelled emissions were nearer to  
618 upper boundaries during years with lower measured emissions (2003, 2004, 2006), and to lower  
619 boundaries during years with higher measured emissions (2007, 2008, 2009). There was no significant  
620 correlation between annual N inputs and measured or modelled emissions. Although annual emissions  
621 in the model were close to 1% of annual N inputs during most years, they were greater in 2008 and  
622 2009 in spite of smaller N inputs because of the large emission events modelled after summer  
623 applications of fertilizer and manure (Fig. 3e,f; Fig. 5h). Annual N inputs (Table 4), supplemented by  
624 3 – 6 g N m<sup>-2</sup> y<sup>-1</sup> modelled from symbiotic fixation by clover [F1 – F26]), were only slightly larger  
625 than annual N removals with harvesting, supplemented by losses of 2 – 3 g N m<sup>-2</sup> y<sup>-1</sup> from all other  
626 gaseous and aqueous emissions (N<sub>2</sub> from denitrification, NH<sub>3</sub> from volatilization, NO<sub>3</sub><sup>-</sup> from  
627 leaching). Consequently residual soil NO<sub>3</sub><sup>-</sup>, while present in the model, did not accumulate during the  
628 study period, and so did not drive increasing N<sub>2</sub>O emissions with sustained N applications. Modelled  
629 and measured annual N<sub>2</sub>O emissions, if expressed in C equivalents (~130 g C g N<sup>-1</sup>), largely offset net  
630 C uptake expressed as NBP (Table 4).

631

632 Increasing harvest intensity and delaying harvest dates had little effect on annual N<sub>2</sub>O  
 633 emissions modelled during the first two years after planting in 2001 and 2008, but raised them  
 634 substantially thereafter (2003 – 2007) (Table 4). During this period, annual emissions rose by an  
 635 average of 24% with increased harvest intensity, and by an average of 43% with increased harvest  
 636 intensity combined with delayed harvest dates. These increases were attributed to reduced N uptake,  
 637 and to increased  $T_s$  and  $\theta$  (Figs. 7, 8).

638

### 639 **Effects of increased bulk density on N<sub>2</sub>O emissions**

640 Increasing near-surface (0 – 3 cm) soil BD by 5% or 10% at the beginning of 2001 in the model  
 641 reduced [O<sub>2(s)</sub>] after rainfall events and slowed recovery of [O<sub>2(s)</sub>] during subsequent drying as shown  
 642 following the manure application in July 2007 (Fig. 9a) and the fertilizer application in late August  
 643 2007 (Fig. 9c). These reductions caused increases in modelled N<sub>2</sub>O effluxes that varied during  
 644 emission events (Fig. 9b,d). Effluxes modelled with increases of 10% in near-surface BD were at times  
 645 double those modelled without (e.g. DOY 201 and 240 in Fig. 9), indicating that relatively small  
 646 changes in soil surface properties could at times cause large changes in emissions. The effects of  
 647 increased BD on modelled  $T_s$ ,  $\theta$ , CO<sub>2</sub> exchange, crop production and N uptake during these events  
 648 were small (results not shown). Increasing near-surface BD by 10% raised annual N<sub>2</sub>O emissions by  
 649 amounts that increased with annual precipitation from *ca.* 10% in drier years (e.g. 2003) to *ca.* 50% in  
 650 wetter (e.g. 2006) (Table 5).

651

### 652 **Effects of Changes in $K_{O_2}$ and $K_{NO_x}$ on N<sub>2</sub>O emissions**

653 Lowering  $K_{O_2}$  to one-half that used in *ecosys* reduced annual N<sub>2</sub>O emissions modelled from  
 654 2004 to 2009 by 16% to an average of 0.218 g N m<sup>-2</sup> y<sup>-1</sup>, near the average lower boundary of the  
 655 measured values (Table 5). Raising  $K_{O_2h}$  to double that used *ecosys* increased these emissions by 28%  
 656 to an average of 0.334 g N m<sup>-2</sup> y<sup>-1</sup>, near the average upper boundary of the measured values. Lowering  
 657  $K_{NO_x}$  to one-half that used in *ecosys* increased annual N<sub>2</sub>O emissions modelled from 2004 to 2009 by  
 658 30% to an average of 0.338 g N m<sup>-2</sup> y<sup>-1</sup>, near the average upper boundary of the measured values  
 659 (Table 5). Raising  $K_{NO_x}$  to double that used *ecosys* reduced these emissions by 27% to an average of  
 660 0.189 g N m<sup>-2</sup> y<sup>-1</sup>, near the average lower boundary of the measured values. In years with lower annual

661 emissions (2003, 2004, 2006 in Table 4), the lower  $K_{O_2}$  or higher  $K_{NO_x}$  gave modelled values that were  
662 closer to measured values. However in years with higher annual emissions (2008 and 2009 in Table 4),  
663 the higher  $K_{O_2}$  or lower  $K_{NO_x}$  gave modelled values that were closer.

664

665

666

## DISCUSSION

667

### Modelled vs. Measured N<sub>2</sub>O Emissions

668

669 Most N<sub>2</sub>O emission events measured from 2004 to 2009 were simulated within the range of  
670 measurement uncertainty, estimated to be about 30% of mean daily values (Fig. 3). However some  
671 deviations between modelled and measured N<sub>2</sub>O emissions were apparent, such as the larger  
672 emissions modelled in autumn 2006 (Fig. 3c) and the smaller emissions modelled in spring 2008 (Fig.  
673 3e). These deviations may be attributed to uncertainties in both the measurements and the model. In  
674 the automated measurement system, the static chambers were rotated about every two months among  
675 fixed positions in a corner of the field. During these periods, surface conditions in the chamber could  
676 deviate from the mean field conditions represented in the model. However we do not have an  
677 explanation for the very small emissions measured after the three manure slurry applications 2006.  
678 The chambers had been removed before the applications and were reinstalled within two hours,  
679 during which the cut grass was removed so that the surface litter in the chambers may have been  
680 reduced from that outside. In the model, emissions following manure or fertilizer applications were  
681 sensitive to the amount of surface litter as noted earlier. The absence of emission events measured  
682 after slurry applications in 2006 was unusual (Fig. 3) given the large precipitation that year (Table 4),  
683 demonstrating that large variability at small spatial scales inevitably affects these measurements. Such  
684 variability adversely affects agreement between modelled and measured emissions (Table 3).

685

686 During spring 2008 sustained emissions of about 5 mg N m<sup>-2</sup> d<sup>-1</sup> were measured by the  
687 chambers in the absence of any manure or fertilizer applications (Fig. 3e). These emissions were  
688 related to the ploughing of the field to a depth of 25cm in December 2007 (Table 2) which hastened  
689 soil organic matter decomposition, and hence N mineralization that increased mineral N substrate for  
690 nitrification and denitrification, and possibly microbial nitrifier and denitrifier populations. These  
691 increases must remain conjectural as the Oensingen study did not include stratified analysis of N<sub>2</sub>O

692 production factors (e.g. microbial biomass, potential denitrification) within the chamber soils.  
693 Although *ecosys* simulates hastened SOM decomposition with tillage (Grant et al., 1998), large  
694 amounts of above- and below-ground plant litter with relatively high C:N ratios were incorporated in  
695 the model with tillage in December 2007 which slowed net N mineralization and hence accumulation  
696 of mineral N products in the model during spring 2008. Consequently modelled N<sub>2</sub>O emissions  
697 remained small until mineral N was raised by fertilizer applications in July (Fig. 3c).

698

### 699 **Modelling Controls on N<sub>2</sub>O Emissions by Litter and Near-Surface $\theta$ and $T_s$**

700 In the model, almost all the N<sub>2</sub>O emissions originated in the surface litter and in the near-  
701 surface (0 – 1 cm) soil layer, so that emissions were strongly controlled by litter and near-surface  $\theta$   
702 and  $T_s$  (Figs. 3 – 4). This model finding is consistent with the experimental finding of Pal et al. (2013)  
703 from <sup>15</sup>N enrichment studies that approximately 70% of N<sub>2</sub>O measured during emission events in a  
704 managed grassland originated in the surface litter. Similarly van der Weerden et al. (2013) inferred  
705 from diurnal variation in  $T_s$  and N<sub>2</sub>O emissions measured after urine amendments on a managed  
706 grassland that N<sub>2</sub>O production was at or near the soil surface (0 - 2 cm). Also Flécharde et al. (2007)  
707 inferred in a meta-analysis of N<sub>2</sub>O emissions from grasslands in Europe that  $\theta$  measured at 5 cm was  
708 not in some cases an adequate scaling factor for N<sub>2</sub>O source strength because N<sub>2</sub>O production and  
709 emission took place at or near the soil surface. *Ecosys* simulated little net production, and even a  
710 small net consumption, of N<sub>2</sub>O in soil below 2 cm during emission events, as may be inferred from  
711 peak [N<sub>2</sub>O<sub>(s)</sub>] modelled in the 0 – 1 cm soil layer and much lower [N<sub>2</sub>O<sub>(s)</sub>] modelled in the 1 – 3 cm  
712 soil layer below (Figs. 3g and 4g). This model finding was consistent with the experimental finding of  
713 Neftel et al. (2000) that N<sub>2</sub>O concentrations below near-surface soil layers in a managed grassland  
714 remained below atmospheric values during emission events, from which they inferred that any N<sub>2</sub>O  
715 generated at depths greater than ~3 cm would not likely reach the soil surface. Thus attempts to relate  
716 N<sub>2</sub>O emissions to  $T_s$  and  $\theta$  measured at greater depths than 3 cm in grasslands are unlikely to be  
717 informative if these differ from near-surface values. These emissions should rather be related to  
718 conditions in the litter and near-surface soil, which need to be better characterized in future studies.

719

720 Consequently modelled N<sub>2</sub>O emissions were highly sensitive to surface wetting and drying (e.g.  
721 Fig. 4e,h) modelled from precipitation vs. ET (e.g. Fig. 4a,c), or to surface warming and cooling (e.g.  
722 Fig. 8j,l) modelled from surface energy balance (e.g. Fig. 4c). The sensitivity to surface wetting and



723 drying was modelled from the effects of  $\theta$  on air- vs. water-filled porosity and hence on diffusivity of  
724 gases in gaseous [D17] and aqueous [D20] phases, and on gaseous volatilization - dissolution transfer  
725 coefficients and hence gas exchange between gaseous and aqueous phases [D14, D15]. These  
726 transfers controlled O<sub>2</sub> supply, and hence demand for alternative e<sup>-</sup> acceptors as the O<sub>2</sub> supply fell  
727 below O<sub>2</sub> demand, which drove N<sub>2</sub>O generation from denitrification [H6 – H8] and nitrification  
728 [H19]. The control of O<sub>2</sub> supply on e<sup>-</sup> acceptors used in nitrification thereby simulated the effect of  
729 WFPS on the fraction of N<sub>2</sub>O generated during nitrification identified by Fang et al. (2015) as  
730 necessary to modelling N<sub>2</sub>O emissions, while avoiding the model-specific parameterization needed in  
731 simpler models. The sensitivity to surface wetting in *ecosys* enabled sharp rises in N<sub>2</sub>O emissions to  
732 be modelled from surface litter and near-surface soil after small precipitation events during DOY 200  
733 - 201 in 2007 (Fig. 4a,h), and after slurry application during DOY 218 in 2009 (Fig. 5a,h), even when  
734 the soil at 5 cm remained dry (Fig. 4b; Fig. 5b). Such rises were consistent with the experimental  
735 findings of Flécharde et al. (2007) that precipitation on dry soil can cause substantial N<sub>2</sub>O emissions  
736 after fertilizer application in grasslands.

737

738 The sensitivity to surface warming and cooling was modelled from the effects of  $T_s$  on  
739 diffusivity of gases in gaseous [D17] and aqueous [D20] phases, and on solubility of gases and hence  
740 exchange of gases between gaseous and aqueous phases [D14, D15], both parameterized from basic  
741 physical relationships independently from the model. These transfers controlled [O<sub>2(s)</sub>] in the surface  
742 litter and soil (Figs. 3f and 4f), and hence O<sub>2</sub> uptake by aerobic heterotrophs [H4] and autotrophs  
743 [H13] through a Michaelis-Menten constant [H4b, H13b]. The sensitivity to surface warming and  
744 cooling was also modelled from the effects of  $T_s$  on SOC oxidation [H2] and hence O<sub>2</sub> demand by  
745 aerobic heterotrophs [H3], and on NH<sub>4</sub><sup>+</sup> and NO<sub>2</sub><sup>-</sup> oxidation [H11, H15] and hence O<sub>2</sub> demand by  
746 aerobic autotrophs [H12, H16]. These effects were driven by a single Arrhenius function used for all  
747 biological transformations [A6] parameterized from basic research conducted independently from the  
748 model. Under sustained high surface  $\theta$ , this combination of physical and biological processes drove  
749 large diurnal variation in N<sub>2</sub>O emissions modelled with diurnal surface warming and cooling during  
750 emission events (e.g. DOY 221 in Fig. 5h, DOY 243 in Fig. 8l), as observed experimentally by van  
751 der Weerden et al. (2013). By explicitly simulating the diverse processes that determine N<sub>2</sub>O  
752 emissions, *ecosys* could model the large sensitivity of emissions to  $T_s$  without the use of  
753 unrealistically large parameters for temperature sensitivity inferred from controlled temperature

754 studies of N<sub>2</sub>O emissions (e.g. Dobbie and Smith, 2001). This large sensitivity to  $T_s$  has been  
755 inadequately represented in simpler models, causing underestimation of large emissions measured  
756 from warm soils (e.g. Saggar et al., 2004). At a seasonal time scale, higher  $T_s$  could cause large  
757 increases in N<sub>2</sub>O emissions modelled with comparable  $\theta$  after the same fertilizer application (Fig. 8l  
758 vs. Fig. 8f). However the effects of  $T_s$  on N<sub>2</sub>O emissions were dominated by those of  $\theta$  during surface  
759 wetting and drying (e.g. Figs. 4h, 7l).

760

761 Values of both  $\theta$  and  $T_s$  thus determined O<sub>2</sub> demand not met by O<sub>2</sub> uptake which drove demand  
762 for alternative e<sup>-</sup> acceptors by heterotrophic denitrifiers [H6] and autotrophic nitrifiers [H19]. This  
763 demand drove the sequential reduction of NO<sub>3</sub><sup>-</sup>, NO<sub>2</sub><sup>-</sup> and N<sub>2</sub>O to NO<sub>2</sub><sup>-</sup>, N<sub>2</sub>O and N<sub>2</sub> respectively by  
764 heterotrophic denitrifiers [H7, H8, H9], and the reduction of NO<sub>2</sub><sup>-</sup> to N<sub>2</sub>O by autotrophic nitrifiers  
765 [H20]. The consequent production of N<sub>2</sub>O (Fig. 4g, Fig. 5g) and N<sub>2</sub> drove emissions of both N<sub>2</sub>O and  
766 N<sub>2</sub> (Fig. 4h, Fig. 5h) through volatilization [D14, D15] and through gaseous and aqueous diffusion  
767 [D16, D19]. Ratios of N<sub>2</sub>O and N<sub>2</sub> emissions in *ecosys* (Fig. 4h, Fig. 5h) were not parameterized as  
768 done in other models, but rather were determined by relative affinities determined from basic research  
769 [H8, H9], and by environmental conditions. When demand from heterotrophic denitrifiers for  
770 alternative e<sup>-</sup> acceptors was small relative to their availability, the preferential reduction of more  
771 oxidized e<sup>-</sup> acceptors generated larger emissions of N<sub>2</sub>O [H7, H8] relative to N<sub>2</sub> [H9]. Such  
772 conditions occurred during the early part of an emission event when surface [NO<sub>3</sub><sup>-</sup>] rose with  
773 nitrification of fertilizer or manure NH<sub>4</sub><sup>+</sup> after application (e.g. DOY 200 – 201 in Fig. 4h). However  
774 when demand for alternative e<sup>-</sup> acceptors was large relative to their availability, this same reduction  
775 sequence forced more rapid reduction of N<sub>2</sub>O to N<sub>2</sub> and hence smaller emissions of N<sub>2</sub>O relative to  
776 N<sub>2</sub>. Such conditions occurred during the later part of emission events when surface [NO<sub>3</sub><sup>-</sup>] declined  
777 with plant uptake (e.g. DOY 202 – 205 in Fig. 4h and DOY 222 in Fig. 5h), or when greater surface  
778 wetting reduced O<sub>2</sub> supply (e.g. DOY 220 in Fig. 5h). This greater demand for alternative e<sup>-</sup> acceptors  
779 with wetting provided a process-based explanation for declines in N<sub>2</sub>O emissions frequently found at  
780 higher  $\theta$  in field studies (e.g. Rafique et al., 2011) without explicit parameterization of N<sub>2</sub>O:N<sub>2</sub> ratios.

781

782 Nitrification and denitrification were also driven by the concentrations of NH<sub>4</sub><sup>+</sup> [H11], NO<sub>3</sub><sup>-</sup>  
783 [H7], NO<sub>2</sub><sup>-</sup> [H8, H15, H20] and N<sub>2</sub>O [H9] relative to Michaelis-Menten constants evaluated from  
784 basic research. The concentrations of NH<sub>4</sub><sup>+</sup> and NO<sub>3</sub><sup>-</sup> in *ecosys* were increased by N additions from

785 manure and fertilizer N applications (Table 2), and by net mineralization soil organic N from  
 786 oxidation of litterfall, manure and SOM [A26] as indicated by soil CO<sub>2</sub> effluxes. These concentrations  
 787 were reduced by root uptake of NH<sub>4</sub><sup>+</sup> and NO<sub>3</sub><sup>-</sup> [C23] and consequent plant N assimilation with  
 788 growth, indicated by more rapid CO<sub>2</sub> fixation with time after cutting (Figs 3 – 4 and Figs. 6 - 7). In  
 789 the model, more rapid CO<sub>2</sub> fixation drove more rapid production of nonstructural C, and hence more  
 790 rapid exchange of nonstructural C and N between canopy and roots [C50], and so hastened root active  
 791 N uptake by increasing  $R_a$  driving root growth [C14b], and by hastening removal of N uptake  
 792 products and hence reducing their inhibition of active uptake [C23g]. The diversity of controls on key  
 793 substrates for N<sub>2</sub>O generation suggests that robust simulations of N<sub>2</sub>O emissions require  
 794 comprehensive ecosystem models in which these controls are fully represented.

### 795 **Modelling Effects of Defoliation Intensity and Timing on N<sub>2</sub>O Emissions**

796  
 797 The control of NH<sub>4</sub><sup>+</sup> and NO<sub>3</sub><sup>-</sup> availability by root N uptake indicated that plant management  
 798 practices determining uptake would thereby affect N<sub>2</sub>O emissions. In the model, increasing harvest  
 799 intensity and delaying harvest dates both slowed N uptake (Fig. 7b,h and Fig. 8b,h) by slowing the  
 800 recovery of LAI (Fig. 6) and CO<sub>2</sub> fixation (Fig. 7a,g and Fig. 8a,g). Both thereby increased [NO<sub>3</sub><sup>-</sup>]  
 801 (Fig. 7c,i and Fig. 8c,i),  $T_s$  (Fig. 7d,j and Fig. 8d,j) and  $\theta$  (Fig. 7e,k and Fig. 8e,k), raising N<sub>2</sub>O  
 802 effluxes modelled during most emission events (Fig. 7f,l and Fig. 8f,l), and hence annually (Table 4).  
 803 This model finding was consistent with the field observations of Jackson et al. (2015) that increased  
 804 N<sub>2</sub>O emissions after defoliation in grasslands were caused by reduced uptake of N and water by  
 805 slower-growing plants.

806  
 807 The effects of defoliation on N<sub>2</sub>O emissions during modelled emission events were similar to,  
 808 or greater than, those of  $T_s$  and  $\theta$  (e.g. Fig. 7f,l), consistent with the experimental finding of Imer et al.  
 809 (2013) that plant management, as represented by its effects on LAI, had a larger effect on N<sub>2</sub>O fluxes  
 810 than did the environment, as represented by  $T_a$ , at an intensively managed grassland in Switzerland.  
 811 Reducing LAI remaining after harvest by one-half and delaying harvest by 5 days had little effect on  
 812 modelled harvest removals (Table 4), suggesting that N<sub>2</sub>O emissions from managed grasslands are  
 813 more sensitive to plant management practices than are yields. Intensity and timing of harvests should  
 814 therefore be selected to avoid slow regrowth of LAI following N additions by avoiding excessive  
 815 defoliation and by allowing as much time as possible between defoliation and subsequent fertilizer or

816 manure application. Neftel et al. (2010) reported enhanced N<sub>2</sub>O emissions after cuts in managed  
817 grassland and hypothesized that a simple mitigation option would be to optimize the timing of the  
818 fertilizer applications. To our knowledge this option has not been systematically investigated.

819

### 820 **Modelling Effects of Soil Bulk Density on N<sub>2</sub>O Emissions**

821 The small increases in near-surface BD included in this study were typical of those arising from  
822 natural variation in soil properties or from compaction by vehicular traffic during field management  
823 operations. In the model, these increases reduced soil porosity and hence gaseous diffusivity [D17]  
824 which slowed O<sub>2</sub> uptake from the atmosphere [D15] and O<sub>2</sub> transfer through the soil profile [D16].  
825 Consequent reductions in near-surface [O<sub>2(s)</sub>] (Fig. 9a,c) slowed O<sub>2</sub> reduction by denitrifiers [H4] and  
826 nitrifiers [H13], forcing more rapid e<sup>-</sup> transfer to NO<sub>3</sub><sup>-</sup> by denitrifiers [H6] and to NO<sub>2</sub><sup>-</sup> by nitrifiers  
827 [H19] and hence more rapid emissions of N<sub>2</sub>O following applications of manure (Fig. 9b) and fertilizer  
828 (Fig. 9d).

829

830 In a study of soil compaction effects on N<sub>2</sub>O emissions from a fertilized agricultural field in a  
831 climate similar to that at Oensingen, Bessou et al. (2010) found that increasing the BD of the upper 30  
832 cm of the soil profile by *ca.* 15% raised annual N<sub>2</sub>O emissions measured with automated chambers by  
833 at least 50% during each of two growing seasons. This rises were similar to that modelled with a  
834 smaller increase in BD of the upper 3 cm during the wettest year of this study (Table 5). During  
835 emission events, Bessou et al. (2010) measured peak fluxes from compacted soil that were double  
836 those from uncompacted, as also modelled here (Fig. 9b,d).

837

838 The detailed algorithms from which *ecosys* was constructed enabled increases in N<sub>2</sub>O  
839 emissions from surface compaction to be simulated from specified changes to surface BD, a  
840 measureable site characteristic, without further model parameterization. The marked increases in N<sub>2</sub>O  
841 emissions modelled with these increases in BD (Table 5) indicated that some of the large spatial  
842 variation in these emissions commonly found in field measurements could arise from relatively small  
843 variation in physical properties of near-surface soil. In future studies of N<sub>2</sub>O emissions, near-surface  
844 soil properties could be determined at each measurement site to establish the extent to which variation  
845 in these properties are associated with those in emissions.

846

### Modelling Effects of $K_{O_2}$ and $K_{NO_x}$ on $N_2O$ Emissions

847  
848  
849  
850  
851  
852  
853  
854  
855  
856  
857  
858  
859  
860  
861  
862  
863  
864  
865  
866  
867  
868  
869  
870  
871  
872  
873  
874  
875

The value of  $K_{O_2}$  used in *ecosys* ( $=2 \mu\text{M}$ ) was taken from the upper range of values determined experimentally for intact cells of heterotrophic bacteria by Longmuir (1954). Halving or doubling  $K_{O_2}$  changed modelled  $N_2O$  emissions (Table 5) by amounts similar to uncertainty in measured emissions expressed as lower and upper boundaries of likely values (Table 4), although the doubled value of  $K_{O_2}$  was larger than those derived from experiments. The value of  $K_{NO_x}$  used in *ecosys* ( $=100 \mu\text{M}$ ) was within the range of values determined experimentally by Yoshinari et al. (1977). As for  $K_{O_2}$ , halving or doubling  $K_{NO_x}$  changed modelled  $N_2O$  emissions (Table 5) by amounts similar to uncertainty in measured emissions expressed as lower and upper boundaries of likely values (Table 4). The halved value of  $K_{NO_x}$  was closer to those measured by Betlach and Tiedje (1981) and Khalil et al. (2007) while the doubled value was closer to that measured by Klemedtsson et al. (1977). These changes indicate that key parameters used in process models must be capable of being constrained by accurate evaluation in independent experiments.

## CONCLUSIONS

$N_2O$  emissions modelled in this managed grassland originated in the surface litter and upper 2 cm of the soil profile. The shallow origin of these emissions enabled *ecosys* to simulate the response of measured emissions to changes in near-surface  $\theta$  and  $T_s$  during brief emission events when rainfall followed manure or mineral fertilizer applications. Measurements of  $\theta$  and  $T_s$  used to estimate  $N_2O$  emissions from managed grasslands should therefore be taken in surface litter and near-surface soil (0 – 2 cm), rather than deeper in the soil profile (5 – 10 cm) as is currently done.

$N_2O$  fluxes modelled during emission events were greater when grassland regrowth and hence mineral N uptake was slower following harvest and subsequent N application. The control of  $N_2O$  emissions by grassland N uptake indicated that  $N_2O$  emissions from managed grassland could be increased by harvesting practices and fertilizer timing that resulted in slower regrowth during periods when emission events are most likely to occur.  $N_2O$  fluxes modelled during emission events rose

876 sharply with small increases in surface BD, indicating the importance of avoiding surface compaction  
877 in fields to which large amounts of N are applied.

878

879 The basic and comprehensive approach to model development in *ecosys* allowed diverse  
880 responses of N<sub>2</sub>O emissions to changes in weather ( $T_s$ ,  $\theta$ ), land management and soil properties to be  
881 modelled from specified changes to readily measured inputs with parameters constrained by basic  
882 experiments conducted independently of the model rather than derived from site-specific observations.  
883 This approach enabled concurrent, well-constrained tests of model performance against a diverse set of  
884 field measurements, and so is expected to confer robustness to the modelling of these emissions under  
885 different climates, soils and land uses in future studies.

886

### 887 **ACKNOWLEDGEMENTS**

888

889 Computational facilities for *ecosys* were provided by the University of Alberta and by the  
890 Compute Canada high performance computing infrastructure. A PC version of *ecosys* with GUI can be  
891 obtained by contacting the corresponding author at [rgrant@ualberta.ca](mailto:rgrant@ualberta.ca). The authors also acknowledge  
892 contributions from valuable discussions with Christoph Amman concerning measurement methodology.

**REFERENCES**

- 893  
894
- 895 Ammann, C., Fléchar, C., Leifeld, J., Neftel, A. and Fuhrer, J.: The carbon budget of newly  
896 established temperate grassland depends on management intensity. *Agriculture, Ecosystems and*  
897 *Environment* 121, 5–20, 2007
- 898 Ammann, C., Spirig, C., Leifeld, J. and Neftel, A.: Assessment of the nitrogen and carbon budget of two  
899 managed temperate grassland fields. *Agriculture, Ecosystems and Environment* 133, 150–162,  
900 2009
- 901 Bessou, C., Mary, B., Léonard, B., Roussel, M., Gréhan, E. and Gabrielle, B.: Modelling soil  
902 compaction impacts on nitrous oxide emissions in arable fields. *Euro. J. Soil Sci.*, 61, 348–363,  
903 2010.
- 904 Betlach, M.R. and Tiedje, J.M.: Kinetic explanation for accumulation of nitrite, nitric oxide, and nitrous  
905 oxide during bacterial denitrification. *Appl. Environ Microbiol.*, 42, 1074-1084, 1981.
- 906 Chatskikh, D.D., Olesen, J.E., Berntsen, J., Regina, K. and Yamulki, S.: Simulation of effects of soils,  
907 climate and management on N<sub>2</sub>O emission from grasslands, *Biogeochem.* 76, 395-419, 2005
- 908 Conant, R.T, Paustian, K., Del Grosso, S.J. and Parton, W.J.: Nitrogen pools and fluxes in grassland  
909 soils sequestering carbon. *Nutr Cycl Agroecosyst* 71, 239–248, 2005.
- 910 Craswell, E. T.: Some factors influencing denitrification and nitrogen immobilization in a clay soil, *Soil*  
911 *Biol. Biochem.* 10, 241-245, 1978
- 912 Dobbie, K.E. and Smith, K.A.: The effect of temperature, water-filled pore space, and land use on N<sub>2</sub>O  
913 emissions from an imperfectly drained gleysol. *Eur. J. Soil Sci.* 52: 667–673, 2001
- 914 Fang, Q.X., Ma, L., Halvorson, A.D., Malone, R.W., Ahuja, L.R., Del Grosso, S.J. and Hatfield, J.L.:  
915 Evaluating four nitrous oxide emission algorithms in response to N rate on an irrigated corn  
916 field. *Environmental Modelling & Software* 72, 56-70, 2015.
- 917 Felber, R., Leifeld, J., Horak J and Neftel, A.: Nitrous oxide emission reduction with greenwaste  
918 biochar: comparison of laboratory and field experiments *Euro. J. Soil Sci.* 65, 128–138 doi:  
919 10.1111/ejss.12093, 2014.
- 920 Fléchar, C.R., Neftel, A., Jocher, M., Ammann, C. and Fuhrer, J.: Bi-directional soil/atmosphere N<sub>2</sub>O  
921 exchange over two mown grassland systems with contrasting management practices. *Glob*  
922 *Change Biol* 11, 2114–2127, 2005.

- 923 Fléchar, C.R., Ambus, P., Skiba, U., Rees, R.M., Hensen, A., van Amstel, A., van den Pol-van  
924 Dasselhaar, A., Soussana, J.-F., Jones, M., Clifton-Brown, J., Raschi, A., Horvath, L., Neftel, A.,  
925 Joher, M., Ammann, C., Leifeld, J., Fuhrer, J., Calanca, P., Thalman, E., Pilegaard, K., Di  
926 Marco, C., Campbell, C., Nemitz, E., Hargreaves, K.J., Levy, P.E., Ball, B.C., Jones, S.K., van  
927 de Bulk, W.C.M., Groot, T., Blom, M., Domingues, R., Kasper, G., Allard, V., Ceschia, E.,  
928 Cellier, P., Laville, P., Henault, C., Bizouard, F., Abdalla, M., Williams, M., Baronti, S.,  
929 Berretti F. and Grosz, B.: Effects of climate and management intensity on nitrous oxide  
930 emissions in grassland systems across Europe, *Agric. Ecosyst. Environ.* 121, 135-152, 2007.
- 931 Grant, R.F.”A review of the Canadian ecosystem model *ecosys*. pp. 173-264 in: *Modeling Carbon and*  
932 *Nitrogen Dynamics for Soil Management*. Shaffer M. (ed). CRC Press. Boca Raton, F, 2001.
- 933 Grant, R.F. Baldocchi, D.D. and Ma, S.: Ecological controls on net ecosystem productivity of a  
934 Mediterranean grassland under current and future climates. *Agric. For Meteorol.* 152: 189– 200,  
935 2012.
- 936 Grant, R.F., Juma, N.G. and McGill, W.B.: Simulation of carbon and nitrogen transformations in soils. I.  
937 Mineralization. *Soil Biol. Biochem.* 27, 1317-1329, 1993a
- 938 Grant, R.F., Juma, N.G. and McGill, W.B.: Simulation of carbon and nitrogen transformations in soils.  
939 II. Microbial biomass and metabolic products. *Soil Biol. Biochem.* 27,1331-1338, 1993b
- 940 Grant, R.F., Izaurrealde, R.C., Nyborg, M., Malhi, S.S., Solberg, E. D. and Jans-Hammermeister, D.:  
941 Modelling tillage and surface residue effects on soil C storage under current vs. elevated CO<sub>2</sub>  
942 and temperature in *ecosys* pp. 527-547 in *Soil Processes and the Carbon Cycle*. Lal, R., Kimble  
943 J.M., Follet, R.F. and Stewart, B.A.(eds). CRC Press. Boca Raton, FL, 1998.
- 944 Grant, R.F. and Pattey, E.: Mathematical modelling of nitrous oxide emissions from an agricultural field  
945 during spring thaw. *Global Biogeochem. Cycles.* 13, 679-694, 1999
- 946 Grant, R.F. and Pattey E.: Modelling variability in N<sub>2</sub>O emissions from fertilized agricultural fields. *Soil*  
947 *Biol. Biochem.* 35, 225-243, 2003.
- 948 Grant, R.F. and Pattey, E.: Temperature sensitivity of N<sub>2</sub>O emissions from fertilized agricultural soils:  
949 mathematical modelling in *ecosys*. *Global Biogeochem. Cycles* 22, GB4019,  
950 doi:10.1029/2008GB003273, 2008.
- 951 Grant, R.F., Pattey, E.M., Goddard, T.W., Kryzanowski, L.M. and Puurveen, H.: Modelling the effects  
952 of fertilizer application rate on nitrous oxide emissions from agricultural fields. *Soil Sci Soc.*  
953 *Amer. J.* 70, 235-248, 2006.



- 954 Imer, D., Merbold, L., Eugster, W. and Buchmann, N.: Temporal and spatial variations of soil CO<sub>2</sub>, CH<sub>4</sub>  
955 and N<sub>2</sub>O fluxes at three differently managed grasslands. *Biogeosci.* 10, 5931–5945, 2013.
- 956 Jackson, R.D., Oates, L.G., Schacht, W.H., Klopfenstein, T.J., Undersander, D.J., Greenquist, M.A.,  
957 Bell, M.M. and Gratton, C.: Nitrous oxide emissions from cool-season pastures under managed  
958 grazing. *Nutr Cycl Agroecosyst* 101, 365–376, 2015.
- 959 Khalil, K., Renault, P., Guérin, N. and Mary, B.: Modelling denitrification including the dynamics of  
960 denitrifiers and their progressive ability to reduce nitrous oxide: comparison with batch  
961 experiments. *Euro. J. Soil Sci.* 56:491–504, 2005.
- 962 Klemetsson, L., Svensson, B.H., Lindberg, T. and Rosswall, T.: The use of acetylene inhibition of  
963 nitrous oxide reductase in quantifying denitrification in soils. *Swedish J. Agric. Res.* 7, 179–185,  
964 1977.
- 965 Longmuir, I.S.: Respiration rate of bacteria as a function of oxygen concentration. *Biochem.* 51, 81-87,  
966 1954.
- 967 Li, Y., Chen, D., Zhang, Y., Edis, R. and Ding, H.: Comparison of three modeling approaches for  
968 simulating denitrification and nitrous oxide emissions from loam-textured arable soils, *Global*  
969 *Biogeochem. Cycles* 19, GB3002, doi:10.1029/2004GB002392, 2005
- 970 Leifeld, J., Ammann, C., Neftel, A. and Fuhrer, J.: A comparison of repeated soil inventory and carbon  
971 flux budget to detect soil carbon changes after conversion from cropland to grasslands. *Global*  
972 *Change Biol.* 17, 3366-3375, 2011
- 973 Lu, Y., Huang, Y., Zou, J. and Zheng, X.: An inventory of N<sub>2</sub>O emissions from agriculture in China  
974 using precipitation-rectified emission factor and background emission, *Chemosphere* 65, 1915-  
975 1924, 2006.
- 976 Metivier, K.A., Pattey, E. and Grant, R.F.: Using the ecosys mathematical model to simulate temporal  
977 variability of nitrous oxide emissions from a fertilized agricultural soil. *Soil Biol. Biochem.* 41,  
978 2370–2386, 2009.
- 979 Neftel, A., Blatter, A., Schmid, M., Lehmann, B. and Tarakanov, S.V.: An experimental determination  
980 of the scale length of N<sub>2</sub>O in the soil of a grassland. *J. Geophys. Res.* 105, 12095–12103, 2000.
- 981 Neftel, A., Ammann, C., Fischer, F., Spirig, C., Conen, F., Emmenegger, L., Tuzson, B. and Wahlen, S.:  
982 N<sub>2</sub>O exchange over managed grassland: Application of a quantum cascade laser spectrometer for  
983 micrometeorological flux measurements *Agric. For. Meteorol.* 150, 775–785, 2010.

- 984 Neftel, A. Spirig, C. and Ammann, C.: Application and test of a simple tool for operational footprint  
985 evaluations. *Environ. Poll.* 152, 644-652, 2008
- 986 Pal, P., Clough, T.J., Kelliher, F.M. and. Sherlock, R.R: Nitrous oxide emissions from in situ deposition  
987 of <sup>15</sup>N-labeled ryegrass litter in a pasture soil. *J. Environ. Qual.* 42, 323-331, 2013
- 988 Pedersen, A.R., Petersen, S.O. and Schelde, K.: A comprehensive approach to soil-atmosphere trace-gas  
989 flux estimation with static chambers. *European Journal of Soil Science*, 61, 888-902, 2010.
- 990 Rafique, R., Hennessy, D. and Kiely, G.: Nitrous oxide emission from grazed grassland under different  
991 management systems. *Ecosystems* 14: 563-582, 2011.
- 992 Ruzjerez, B.E., White, R.E. and Ball, P.R.: Long-term measurement of denitrification in three  
993 contrasting pastures grazed by sheep. *Soil Biol Biochem* 26:29-39, 1994.
- 994 Saggar, S., Andrew, R.M., Tate, K.R., Hedley, C.B., Rodda, N.J. and Townsend, J.A.: Modelling nitrous  
995 oxide emissions from dairy-grazed pastures. *Nutr. Cycl. Agroecosyst* 68:243-255, 2004
- 996 Saxton, K.E., Rawls, W.J., Romberger, J.S. and Papendick, R. I.: Estimating generalized soil-water  
997 characteristics from texture. *Soil Sci. Soc. Amer. J.* 50(4), 1031-1036, 1986.
- 998 Saxton, K.E. and Rawls, W.J.: Soil water characteristic estimates by texture and organic matter for  
999 hydrologic solutions. *Soil Sci. Soc. Am. J.* 70, 1569-1578, 2006.
- 1000 Schmid, M., Neftel, A., Riedo, M. and Fuhrer, J.: Process-based modelling of nitrous oxide emissions  
1001 from different nitrogen sources in mown grassland. *Nutr. Cycl. Agroecosyst.* 60, 177-187, 2001.
- 1002 Smith, K.A. and Massheder, J.: Predicting nitrous oxide emissions from N-fertilized grassland soils in  
1003 the UK from three soil variables, using the B-LINE 2 model. *Nutr Cycl Agroecosyst* 98, 309-  
1004 326, 2014.
- 1005 van der Weerden, T.J., Clough, T.J. and Styles, T.M.: Using near-continuous measurements of N<sub>2</sub>O  
1006 emission from urine-affected soil to guide manual gas sampling regimes. *New Zealand J. Agric.*  
1007 *Res.* 56, 60-76, 2013.
- 1008 Yoshinari. T., Hynes, R. and Knowles, R.: Acetylene inhibition of nitrous oxide reduction and  
1009 measurement of denitrification and nitrogen fixation in soil. *Soil Biol. Biochem.* 9, 177-183,  
1010 1977.
- 1011
- 1012
- 1013
- 1014

1015 **Table 1.** Key soil properties of the Eutri-Stagnic Cambisol at Oensingen as used in *ecosys*.

Depth	BD <sup>¶</sup>	TOC	TON	FC <sup>†</sup>	WP <sup>†</sup>	K <sub>sat</sub> <sup>†</sup>	pH	Sand <sup>‡</sup>	Silt <sup>‡</sup>	Clay <sup>‡</sup>	CF
m	Mg m <sup>-3</sup>	g kg <sup>-1</sup>	g kg <sup>-1</sup>	m <sup>3</sup> m <sup>-3</sup>	m <sup>3</sup> m <sup>-3</sup>	mm h <sup>-1</sup>		g kg <sup>-1</sup>	g kg <sup>-1</sup>	g kg <sup>-1</sup>	m <sup>3</sup> m <sup>-3</sup>
0.01	1.21	27.2	2.9	0.38	0.22	3.4	7	240	330	430	0
0.03	1.21	27.2	2.9	0.38	0.22	3.4	7	240	330	430	0
0.07	1.21	27.2	2.9	0.38	0.22	3.4	7	240	330	430	0
0.13	1.24	27.2	2.9	0.39	0.23	3.4	7	240	330	430	0
0.28	1.28	20.2	2.1	0.40	0.24	2.4	7	180	380	440	0
0.6	1.28	11.6	1.1	0.40	0.24	1.4	7	180	380	440	0
0.7	1.28	11.6	1.1	0.40	0.24	1.4	7	180	380	440	0
0.9	1.28	9	0.9	0.40	0.24	1.4	7	180	380	440	0
1.5	1.28	6	0.6	0.40	0.24	1.4	7	180	380	440	0.1

1016 <sup>¶</sup>abbreviations BD: bulk density, TOC and TON: total organic C and N, FC: field capacity, WP: wilting  
1017 point, K<sub>sat</sub>: saturated hydraulic conductivity, CF: coarse fragments.

1018 <sup>‡</sup>BD, TOC and texture were determined from soil cores taken in 2001 and 2006. Details are given in  
1019 Leifeld et al. (2011).

1020 <sup>†</sup>FC, WP and K<sub>sat</sub> were estimated from BD, TOC and texture according to Saxton et al. (1996) and  
1021 Saxton and Rawls (2006).

1022

1023

1024

**Table 2.** Plant and soil management operations at the Oensingen intensively managed grassland from 2001 to 2009.

Year	Plant Management		Soil Management					
	Date	Management	Date	Management	Amount (g m <sup>-2</sup> )			
					NH <sub>4</sub> <sup>+</sup>	NO <sub>3</sub> <sup>-</sup>	ON	OC
2001			07 May	tillage				
			10 May	tillage				
	11 May	planting	15 June	mineral fertilizer	1.5	1.5		
	1 July	harvest	12 July	mineral fertilizer	1.5	1.5		
	8 Aug.	harvest	16 Aug.	mineral fertilizer	1.15	1.15		
	12 Sep.	harvest						
	31 Oct.	harvest						
2002			12 Mar.	mineral fertilizer	1.5	1.5		
	15 May	harvest	22 May	manure slurry	4.2		2.8	31.2
	25 June	harvest	1 July	mineral fertilizer	1.75	1.75		
	15 Aug.	harvest	18 Aug.	manure slurry	5.9		5.3	49.6
	18 Sep.	harvest	30 Sep.	mineral fertilizer	1.5	1.5		
	07 Dec.	harvest						
2003			18 Mar.	manure slurry	5.9		5.3	61.1
	30 May	harvest	02 June	mineral fertilizer	1.5	1.5		
	04 Aug.	harvest	18 Aug.	manure slurry	6.3		1.9	19.0
	13 Oct.	harvest						
2004			17 Mar.	manure slurry	5.0		1.5	19.5
	11 May	harvest	17 May	mineral fertilizer	1.5	1.5		
	25 June	harvest	01 July	manure slurry	5.5		0.5	9.9
	28 Aug.	harvest	31 Aug.	mineral fertilizer	1.5	1.5		
	03 Nov.	harvest						
2005			29 Mar.	manure slurry	6.7		3.1	42.0
	10 May	harvest	17 May	mineral fertilizer	1.5	1.5		
	27 June	harvest	05 July	manure slurry	5.0		3.5	59.6
	29 Aug.	harvest	16 Sep.	mineral fertilizer	1.5	1.5		
	24 Oct.	harvest						
2006	24 May	harvest						
	05 July	harvest	13 July	manure slurry	4.7		1.4	12.5
	12 Sep.	harvest	27 Sep.	manure slurry	4.4		1.3	13.6
	26 Oct.	harvest	30 Oct.	manure slurry	6.4		3.2	57.8

2007			03 Apr.	manure slurry	5.2		4.6	75.1
	26 Apr.	harvest	03 May	mineral fertilizer	1.5	1.5		
	06 July	harvest	13 July	manure slurry	4.9		1.8	45.9
	23 Aug.	harvest	28 Aug.	mineral fertilizer	1.5	1.5		
	11 Oct.	harvest	24 Oct.	manure slurry	4.6		3.0	38.9
	19 Dec.	terminate	19 Dec.	plowing				
2008			01 May	tillage				
			04 May	tillage				
	05 May	planting						
	01 July	harvest	10 July	mineral fertilizer	1.5	1.5		
	29 July	harvest	07 Aug.	mineral fertilizer	1.5	1.5		
	08 Sep.	harvest	19 Sep.	manure slurry	2.9		0.5	8.6
	07 Nov.	harvest						
2009			07 Apr.	mineral fertilizer	1.5	1.5		
	01 May	harvest	12 May	manure slurry	4.4		1.6	26.0
	16 June	harvest	06 Aug.	manure slurry	3.3		1.2	19.0
	29 July	harvest						
	07 Sep.	harvest	15 Sep.	mineral fertilizer	6.5(urea)			
	20 Oct.	harvest						

**Table 3:** Intercepts (*a*), slopes (*b*) coefficients of determination ( $R^2$ ), ratios of mean squares for regression vs. error (F) and number of data pairs from regressions of log-transformed 4-hour averages of N<sub>2</sub>O fluxes modelled vs. measured at the Oensingen intensively managed grassland from 2004 to 2009.

Year	<i>a</i>	<i>b</i>	$R^2$	F <sup>†</sup>	<i>n</i>
2004	$1.25 \pm 0.88 \times 10^{-5}$	$0.49 \pm 0.06$	0.08	69	818
2005	$1.63 \pm 0.43 \times 10^{-5}$	$0.59 \pm 0.03$	0.24	368	1173
2006	$4.28 \pm 0.44 \times 10^{-5}$	$1.04 \pm 0.08$	0.14	155	948
2007	$1.21 \pm 0.33 \times 10^{-5}$	$0.67 \pm 0.02$	0.35	989	1794
2008	$1.44 \pm 0.51 \times 10^{-5}$	$0.44 \pm 0.03$	0.08	157	1703
2009	$-0.03 \pm 0.25 \times 10^{-5}$	$0.71 \pm 0.02$	0.49	1574	1614

<sup>†</sup> All values of F were highly significant ( $P < 0.001$ ).

**Table 4.** Annual gross primary productivity (GPP), ecosystem respiration ( $R_e$ ), net ecosystem productivity (NEP = GPP -  $R_e$ ), harvest, net biome productivity (NBP) and N<sub>2</sub>O emissions derived from EC or chambers and modelled (M) with current land management (Table 2), and with defoliation increased so that LAI remaining after harvesting was reduced by one-half (1/2), with defoliation increased and delayed by 5 days (1/2 + 5d). Positive values indicate uptake, negative values emissions.

Year		2002	2003	2004	2005	2006	2007	2008	2009
Precip.(mm)		1478	817	1158	966	1566	1328	1188	1004
MAT (°C)		9.56	9.58	8.92	8.67	9.30	9.59	9.30	9.48
GPP	EC	2159	1773	2058	1766	1817	2102	1455	2119
(g C m <sup>-2</sup> y <sup>-1</sup> )	M: current	2214	1836	2220	2111	1953	2539	1419	1852
	: 1/2	2064	1764	2054	1969	1865	2285	1305	1705
	: 1/2 + 5d	2014	1774	2076	1966	1771	2277	1225	1686
$R_e$	EC	-1490	-1558	-1541	-1565	-1577	-1684	-1450	-1657
(g C m <sup>-2</sup> y <sup>-1</sup> )	M: current	-1560	-1421	-1704	-1679	-1680	-1935	-1366	-1373
	: 1/2	-1457	-1345	-1569	-1572	-1579	-1714	-1212	-1259
	: 1/2 + 5d	-1458	-1350	-1541	-1517	-1519	-1679	-1183	-1235
NEP	EC	669	215	517	201	240	418	5	462
(g C m <sup>-2</sup> y <sup>-1</sup> )	M: current	654	415	516	432	273	604	53	479
	: 1/2	607	419	485	397	286	571	93	446
	: 1/2 + 5d	556	414	535	449	252	598	42	451
Harvest	field	462	241	401	247	232	448	293	532
(g C m <sup>-2</sup> y <sup>-1</sup> )	M: current	570	314	525	460	421	690	308	487
	: 1/2	561	360	465	497	455	678	314	484
	: 1/2 + 5d	537	353	579	513	446	686	262	473
C inputs		81	80	29	102	84	160	9	45
NBP	field	288	54	145	56	92	130	-279	-25
(g C m <sup>-2</sup> y <sup>-1</sup> )	M: current	165	181	20	74	-64	74	-246	37
	: 1/2	127	139	49	2	-85	53	-212	7
	: 1/2 + 5d	101	141	-15	38	-110	72	-211	23
N inputs		27.6	22.5	18.5	24.3	21.4	30.1	9.4	20.0
N <sub>2</sub> O	chamber								
(g N m <sup>-2</sup> y <sup>-1</sup> )	upper bound	-0.130	-0.050	-0.060	-0.230	-0.020	-0.280	-0.480	-0.510
	lower bound	-0.450	-0.180	-0.180	-0.320	-0.060	-0.350	-0.620	-0.680
	M: current	-0.302	-0.209	-0.183	-0.193	-0.220	-0.281	-0.326	-0.366
	: 1/2	-0.269	-0.215	-0.250	-0.249	-0.318	-0.312	-0.335	-0.318
	: 1/2 + 5d	-0.284	-0.234	-0.347	-0.352	-0.273	-0.348	-0.327	-0.395

**Table 5.** Annual N<sub>2</sub>O emissions modelled with current field management (Table 2) and soil properties (Table 1) (current), with soil bulk density (BD) increased by 5% and 10% to a depth of 3 cm, and with the Michaelis-Menten constants for reduction of O<sub>2</sub> ( $K_{O_2}$ ) and of NO<sub>3</sub><sup>-</sup> and NO<sub>2</sub><sup>-</sup> ( $K_{NO_x}$ ) halved or doubled from those used in the model.

Year		2002	2003	2004	2005	2006	2007	2008	2009
Precip.(mm)		1478	817	1158	966	1566	1328	1188	1004
MAT (°C)		9.56	9.58	8.92	8.67	9.30	9.59	9.30	9.48
N <sub>2</sub> O (g N m <sup>-2</sup> y <sup>-1</sup> )	current	-0.302	-0.209	-0.183	-0.193	-0.220	-0.281	-0.326	-0.366
	BD + 5%	-0.352	-0.213	-0.218	-0.199	-0.309	-0.332	-0.358	-0.372
	BD + 10%	-0.334	-0.235	-0.231	-0.236	-0.336	-0.374	-0.424	-0.371
	$K_{O_2} \times 0.5$	-0.250	-0.179	-0.154	-0.159	-0.160	-0.216	-0.276	-0.349
	$K_{O_2} \times 2.0$	-0.390	-0.263	-0.221	-0.247	-0.315	-0.385	-0.381	-0.468
	$K_{NO_x} \times 0.5$	-0.382	-0.261	-0.265	-0.267	-0.262	-0.378	-0.432	-0.457
	$K_{NO_x} \times 2.0$	-0.234	-0.163	-0.126	-0.132	-0.126	-0.208	-0.232	-0.288



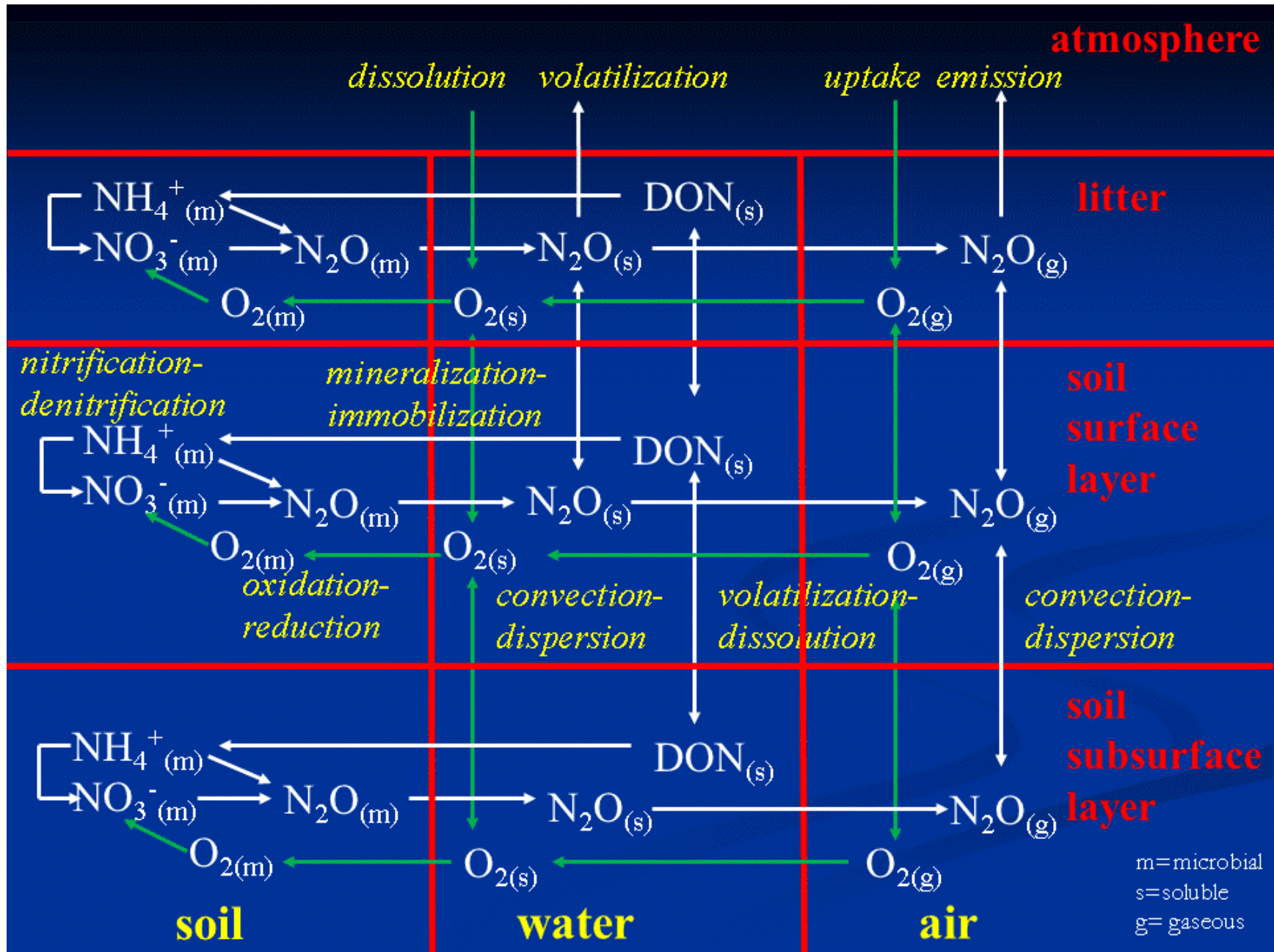


**Fig. 1:** Summary of key processes governing generation and emission of  $N_2O$  as represented in *ecosys*.

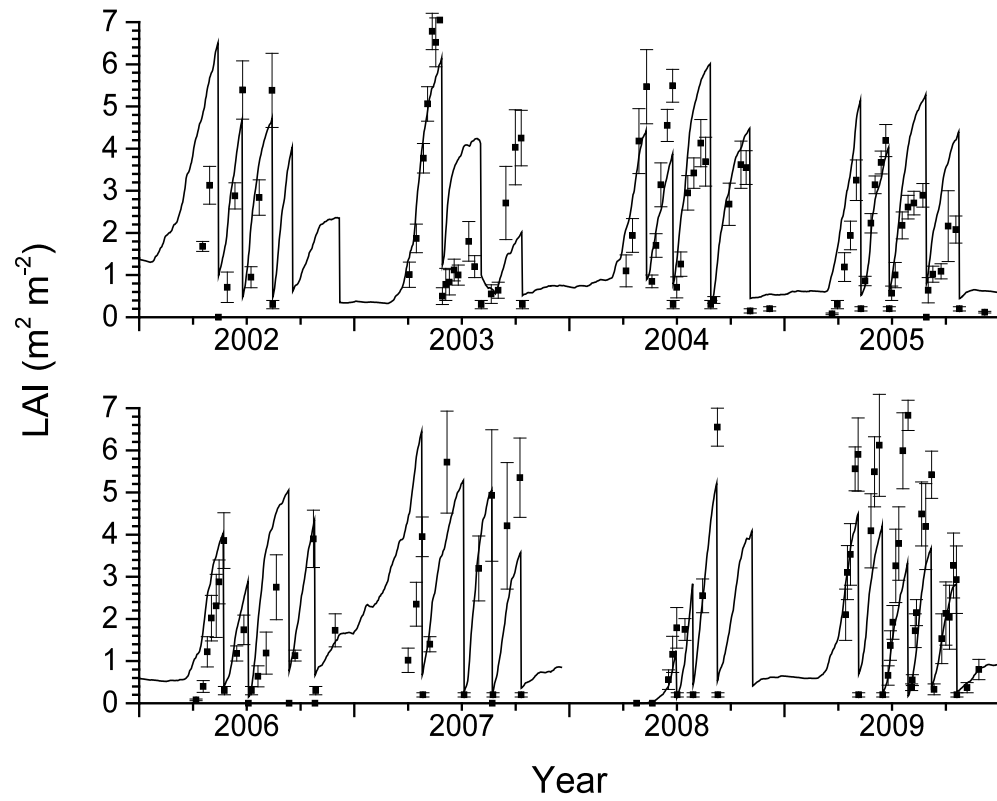


**Fig. 2.** LAI measured (symbols) and modelled (lines) from 2002 through 2009 at the Oensingen intensively managed grassland.

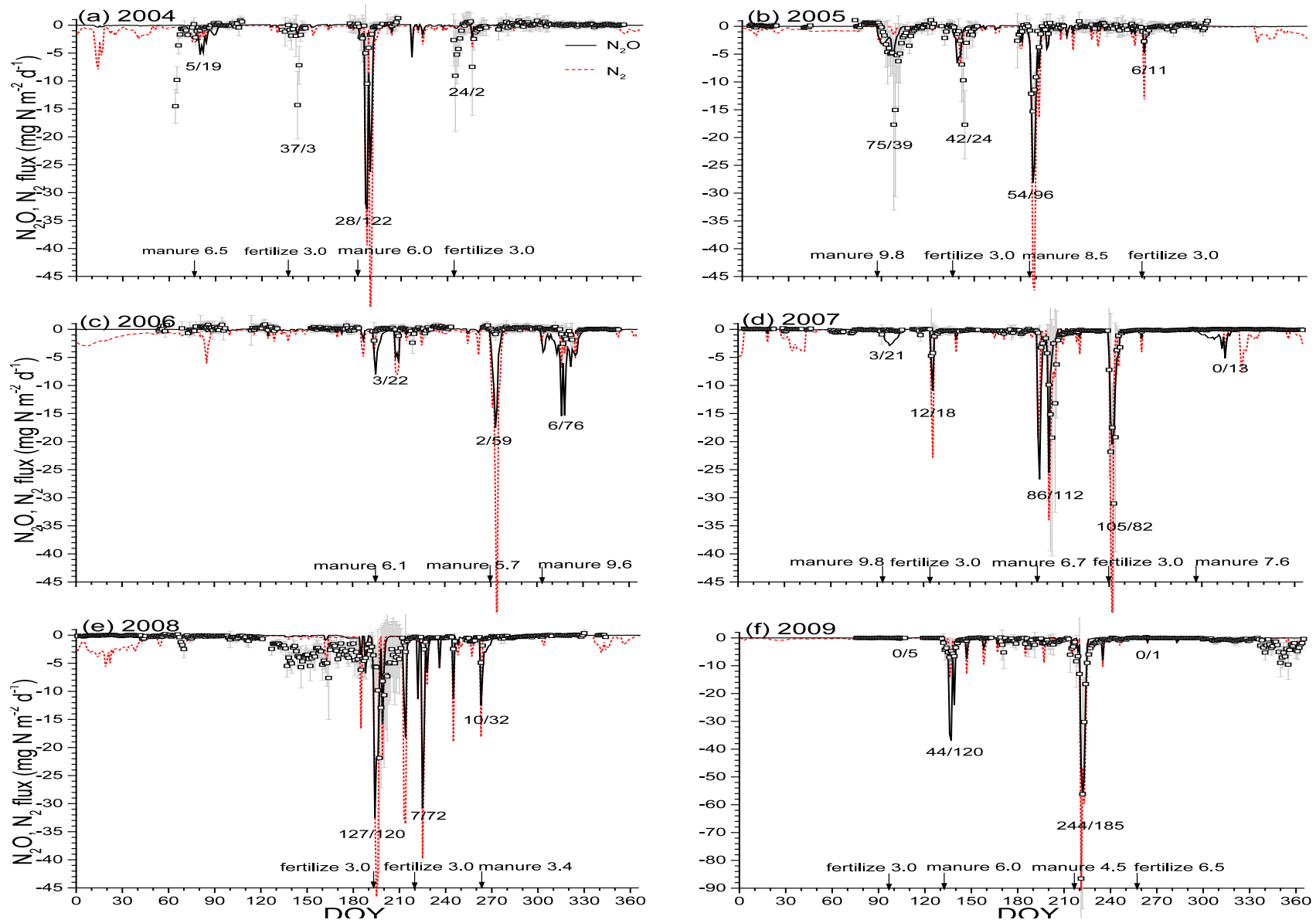


**Fig. 3.** Daily-aggregated  $\text{N}_2\text{O}$  emissions measured (symbols) and  $\text{N}_2\text{O}$  and  $\text{N}_2$  emissions modelled (lines) from 2004 through 2009 at the Oensingen intensively managed grassland. Numbers above and beside each fertilizer or manure addition indicate total measured/modelled  $\text{N}_2\text{O}$ -N emitted during emission events ( $\text{mg N m}^{-2}$ ), and total N applied ( $\text{g N m}^{-2}$ ). Negative values indicate effluxes to the atmosphere.

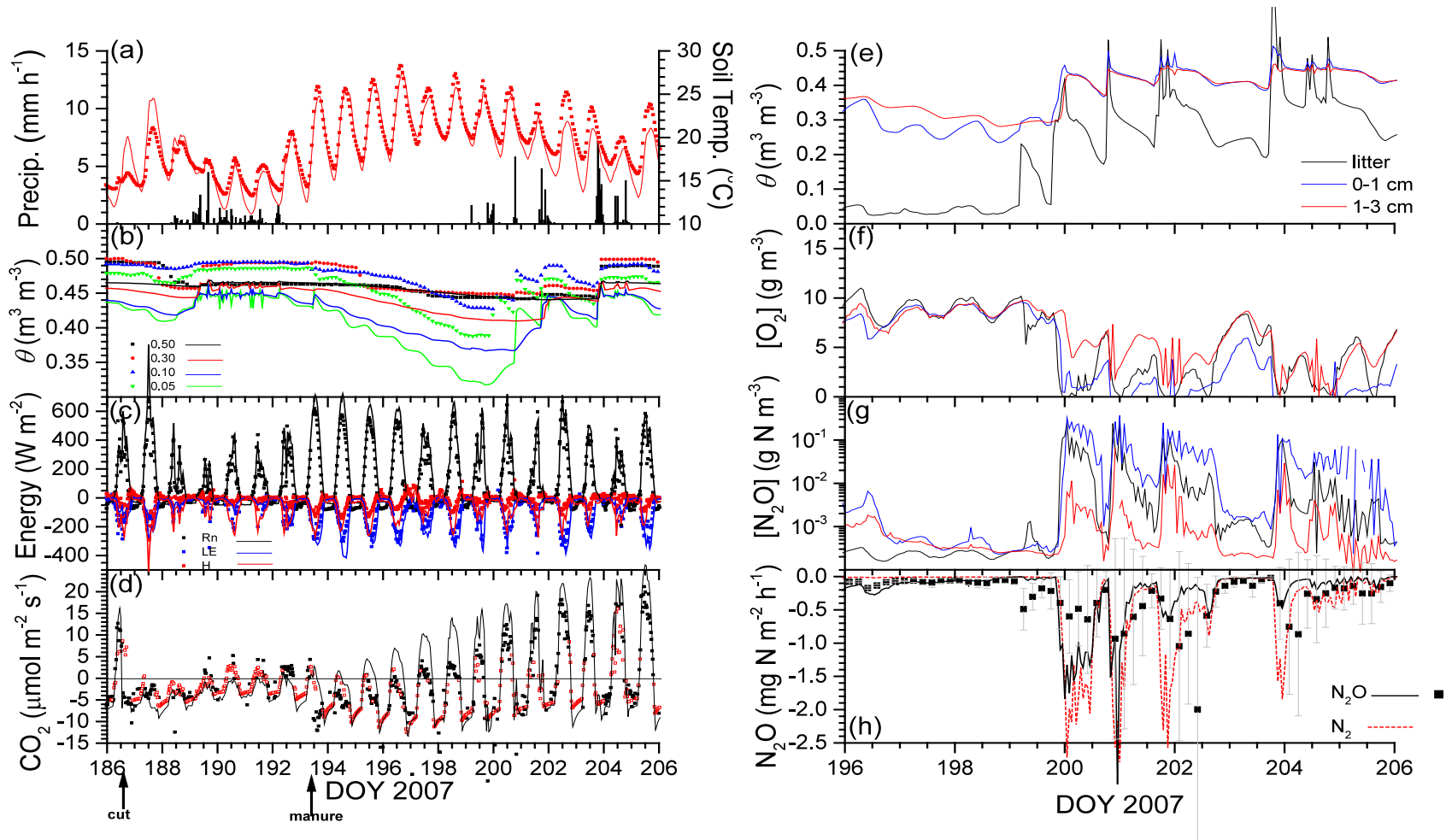


**Fig. 4.** (a) Precipitation and soil temperature at 0.05 m, (b) soil water content ( $\theta$ ) at 0.05, 0.10, 0.30 and 0.50 m, (c) energy and (d) CO<sub>2</sub> fluxes measured (closed symbols), gap-filled (open symbols) and modelled (lines) during 20 days from harvest (cut) to the end of the emission event following manure application (manure) in July 2007. (e)  $\theta$ , (f and g) aqueous concentrations of O<sub>2</sub> and N<sub>2</sub>O modelled in the surface litter and at 0.01 and 0.02 m in the soil, and (h) N<sub>2</sub>O and N<sub>2</sub> fluxes measured (symbols) and modelled (lines) during the last 10 days of this period when the emission event occurred. For fluxes, positive values represent influxes to the soil, negative values effluxes to the atmosphere.

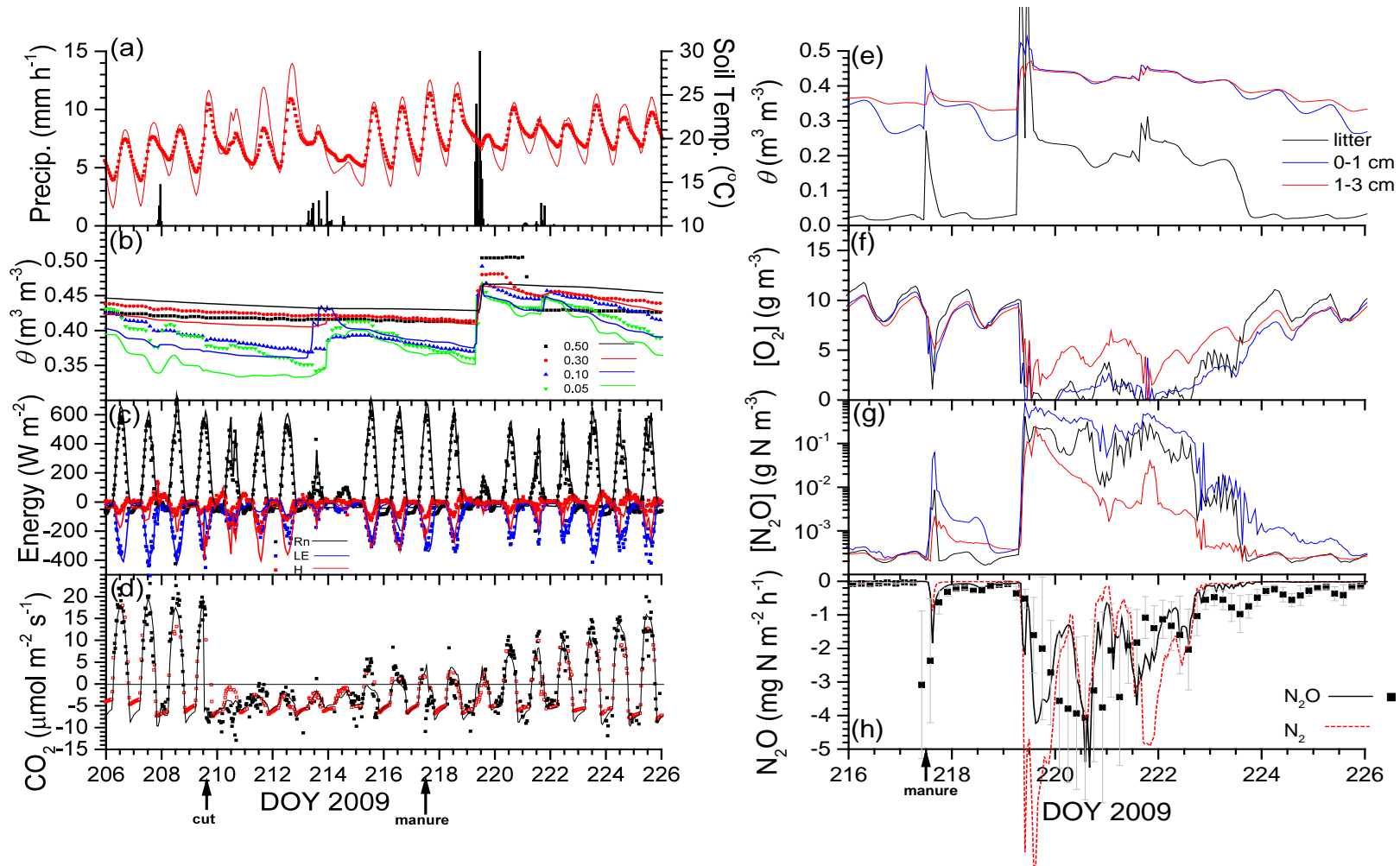


**Fig. 5.** (a) Precipitation and soil temperature at 0.05 m, (b) soil water content ( $\theta$ ) at 0.05, 0.10, 0.30 and 0.50 m, (c) energy and (d) CO<sub>2</sub> fluxes measured (closed symbols), gap-filled (open symbols) and modelled (lines) during 20 days from harvest (cut) to the end of the emission event following manure application (manure) in August 2008. (e)  $\theta$ , (f and g) aqueous concentrations of O<sub>2</sub> and N<sub>2</sub>O modelled in the surface litter and at 0.01 and 0.02 m in the soil, and (h) N<sub>2</sub>O and N<sub>2</sub> fluxes measured (symbols) and modelled (lines) during the last 10 days of this period when the emission event occurred. Positive flux values represent influxes to the soil, negative values effluxes to the atmosphere.

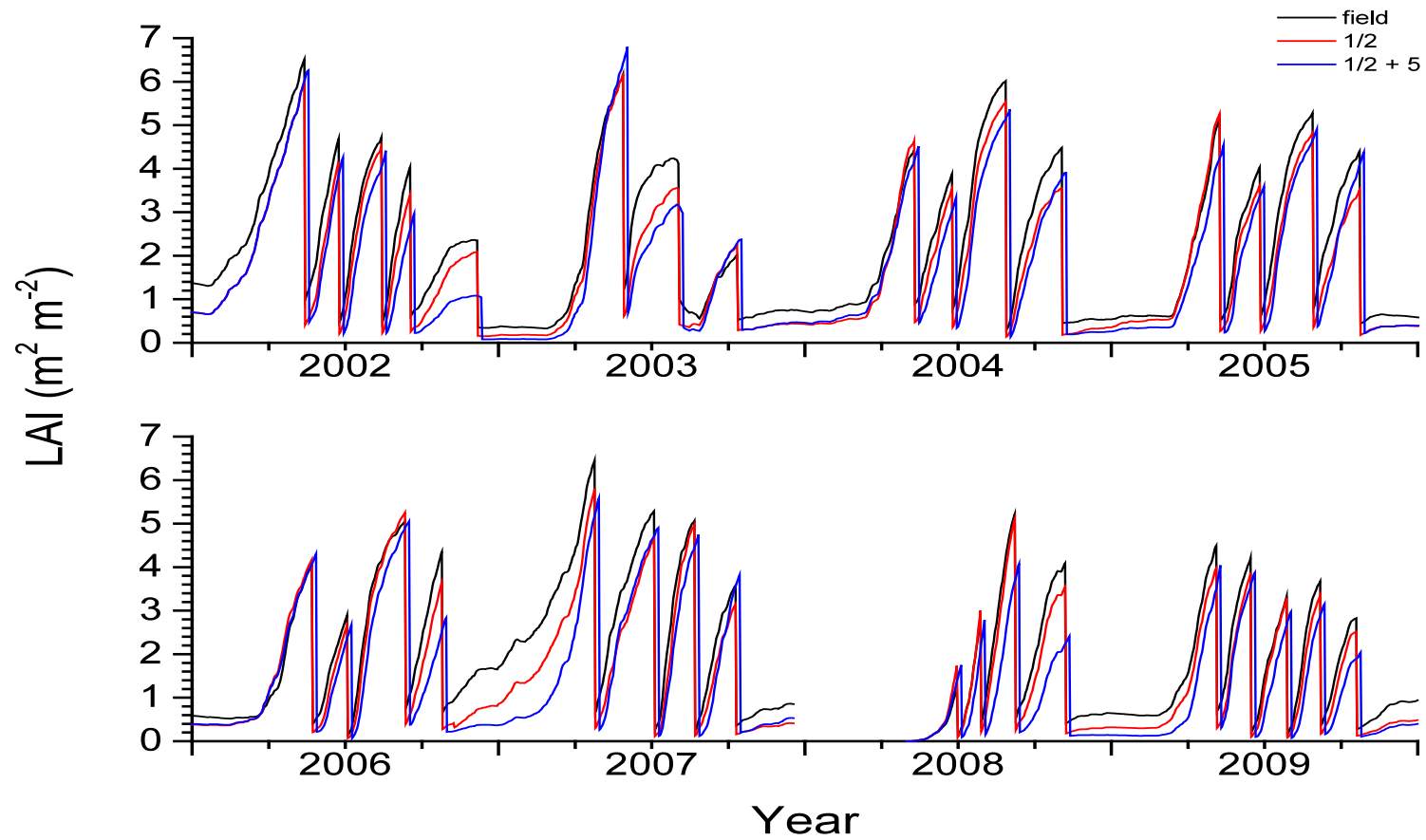


**Fig. 6.** LAI modelled from 2002 through 2009, with LAI after each cut reduced to one-half of that estimated from the field experiment without or with a delay of 5 days at the Oensingen intensively managed grassland.

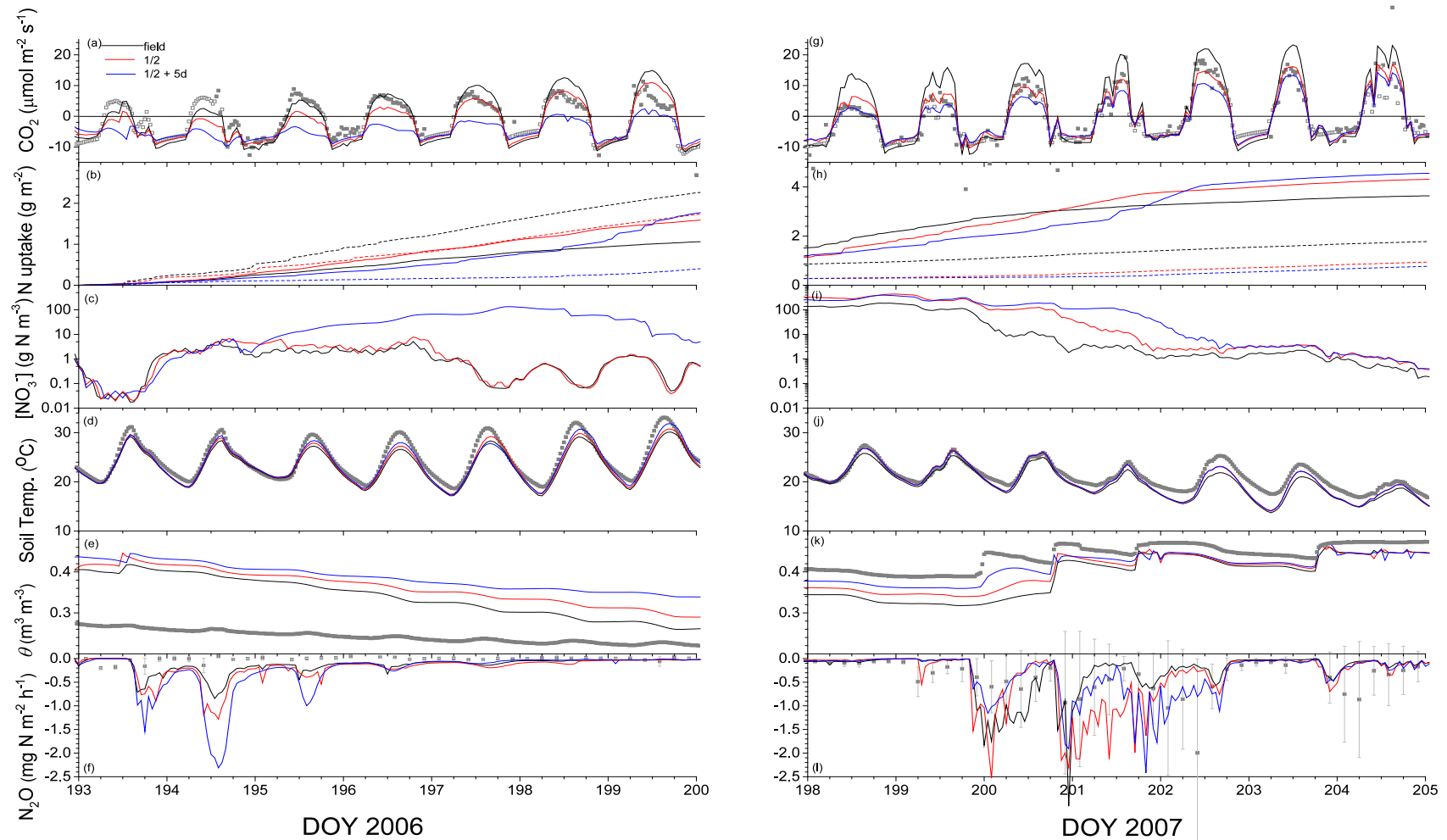


**Fig. 7.** (a,g)  $\text{CO}_2$  fluxes, (b,h) cumulative  $\text{NH}_4^+$  (dashed) and  $\text{NO}_3^-$  (solid) uptake since manure application, (c,i) aqueous  $\text{NO}_3^-$  concentrations at 0 – 1 cm, (d,j)  $T_s$  and (e,k)  $\theta$  at 5 cm, and (f,l)  $\text{N}_2\text{O}$  fluxes measured (symbols) and modelled (lines) with LAI after each cut reduced to one-half of that estimated from the field experiment without or with a delay of 5 days during emission events following manure applications on DOY 194 in (a-f) 2006 and (g-l) 2007 (see Table 2). For fluxes, positive values represent influxes to the soil, negative values effluxes to the atmosphere.

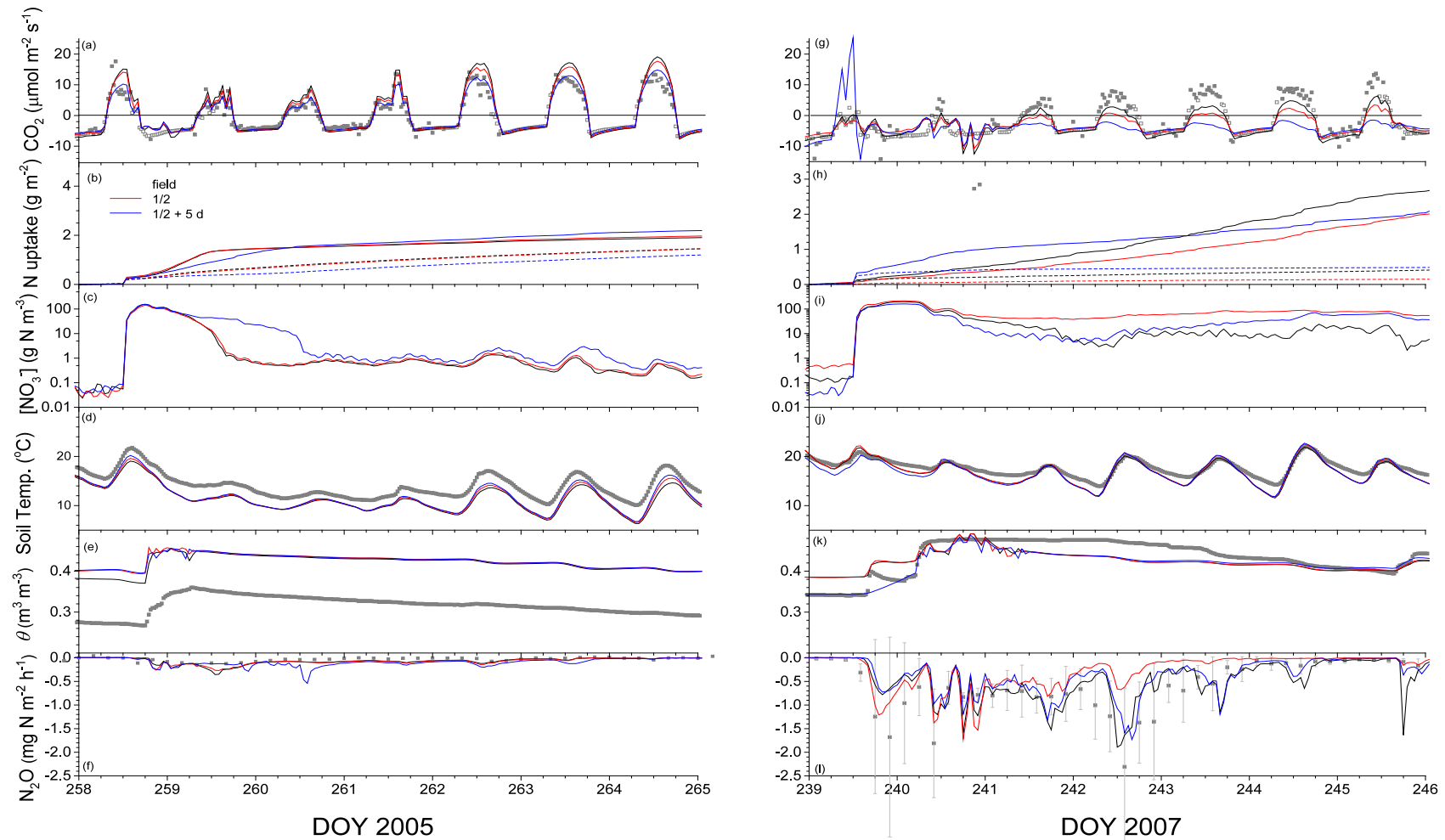


**Fig. 8** (a,g)  $\text{CO}_2$  fluxes, (b,h) cumulative  $\text{NH}_4^+$  (dashed) and  $\text{NO}_3^-$  (solid) uptake since fertilizer application, (c,i) aqueous  $\text{NO}_3^-$  concentrations at 0 – 1 cm, (d,j)  $T_s$  and (e,k)  $\theta$  at 5 cm, and (f,l)  $\text{N}_2\text{O}$  fluxes measured (symbols) and modelled (lines) with LAI after each cut reduced to one-half of that estimated from the field experiment without or with a delay of 5 days during emission events following fertilizer applications on DOY 259 in 2005 (a-f) and DOY 240 in 2007 (g-l) (see Table 2). For fluxes, positive values represent influxes to the soil, negative values effluxes to the atmosphere.



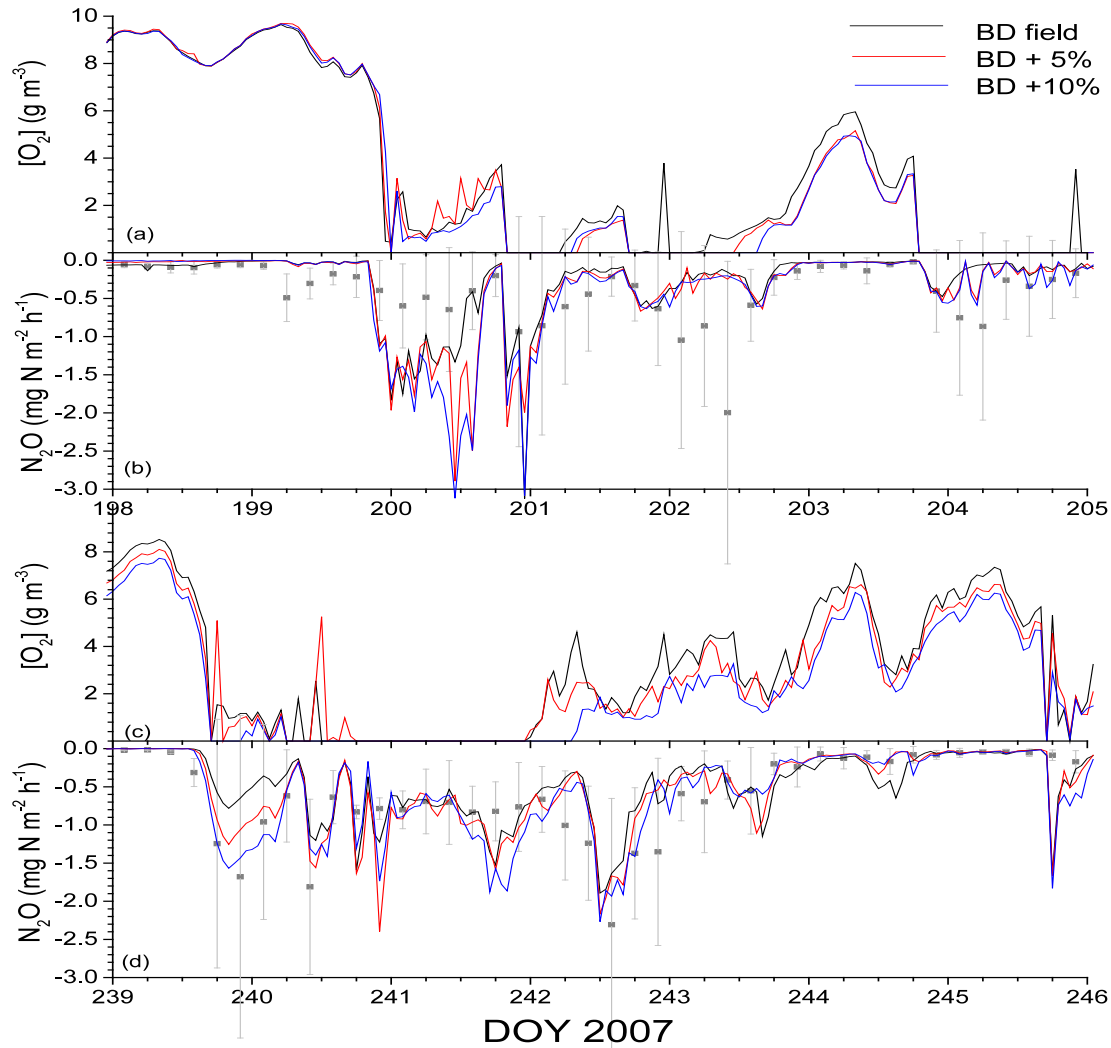


**Fig. 9.** (a,c) Aqueous  $O_2$  concentrations, and (b,d)  $N_2O$  fluxes measured (symbols) and modelled (lines) with bulk density (BD) from field measurements, and with BD raised by 5% or 10% following (a,b) manure application on DOY 194 and (c,d) fertilizer application on DOY 240 in 2007 (see Table 2). For fluxes, positive values represent influxes to the soil, negative values effluxes to the atmosphere.